Natural Environment Research Council

Institute of Geological Sciences

Mineral Reconnaissance Programme Report

A report prepared for the Department of Industry

D. Ostle
Programme Manager
Institute of Geological Sciences
Keyworth,
Nottingham NG12 5GG

No. 56

Geophysical and geochemical investigations over the Long Rake, Haddon Fields, Derbyshire

INSTITUTE OF GEOLOGICAL SCIENCES

Natural Environment Research Council

Mineral Reconnaissance Programme

Report No. 56

Geophysical and geochemical investigations over the Long Rake, Haddon Fields, Derbyshire

Geochemistry
M. J. Brown, BSc

Geophysics
R. D. Ogilvy, MSc

London 1982

A report prepared for the Department of Industry

Mineral Reconnaissance Programme Reports

10 Geophysical surveys around Talnotry mine, Kirkcudbrightshire, Scotland

11 A study of the space form of the Cornubian granite batholith and its application to detailed gravity surveys in Cornwall

12 Mineral investigations in the Teign Valley, Devon. Part 1—Barytes

13 Investigation of stratiform sulphide mineralisation at McPhun's Cairn, Argyllshire

14 Mineral investigations at Woodhall and Longlands in north Cumbria

15 Investigation of stratiform sulphide mineralisation at Meall Mor, South Knapdale, Argyll

16 Report on geophysical and geological surveys at Blackmount, Argyllshire

17 Lead, zinc and copper mineralisation in basal Carboniferous rocks at Westwater, south Scotland

18 A mineral reconnaissance survey of the Doon–Glenkens area, south-west Scotland

19 A reconnaissance geochemical drainage survey of the Criffel–Dalbeattie granodiorite complex and its environs

20 Geophysical field techniques for mineral exploration

21 A geochemical drainage survey of the Fleet granitic complex and its environs

22 Geochemical and geophysical investigations north-west of Llanrwst, North Wales

23 Disseminated sulphide mineralisation at Garbh Achadh, Argyllshire, Scotland

24 Geophysical investigations along parts of the Dent and Augill Faults

25 Mineral investigations near Bodmin, Cornwall. Part 1–Airborne and ground geophysical surveys

26 Stratabound barium-zinc mineralisation in Dalradian schist near Aberfeldy, Scotland: Preliminary report

27 Airborne geophysical survey of part of Anglesey, North Wales

28 A mineral reconnaissance survey of the Abington–Biggar–Moffat area, south-central Scotland

29 Mineral exploration in the Harlech Dome, North Wales

30 Porphyry style copper mineralisation at Black Stockarton Moor,south-west Scotland

31 Geophysical investigations in the Closehouse–Lunedale area

32 Investigations at Polyphant, near Launceston, Cornwall

33 Mineral investigations at Carrock Fell, Cumbria. Part 1–Geophysical survey

34 Results of a gravity survey of the south-west margin of Dartmoor, Devon

35 Geophysical investigation of chromite-bearing ultrabasic rocks in the Baltasound–Hagdale area, Unst, Shetland Islands

36 An appraisal of the VLF ground resistivity technique as an aid to mineral exploration

37 Compilation of stratabound mineralisation in the Scottish Caledonides

38 Geophysical evidence for a concealed eastern extension of the Tanygrisiau microgranite and its possible relationship to mineralisation

39 Copper-bearing intrusive rocks at Cairngarroch Bay, south-west Scotland

40 Stratabound barium-zinc mineralisation in Dalradian schist near Aberfeldy, Scotland: Final report

41 Metalliferous mineralisation near Lutton, Ivybridge, Devon

42 Mineral exploration in the area around Culvennan Fell, Kirkcowan, south-western Scotland

43 Disseminated copper-molybdenum mineralisation near Ballachulish, Highland Region

44 Reconnaissance geochemical maps of parts of south Devon and Cornwall

45 Mineral investigatons near Bodmin, Cornwall. Part 2 New uranium, tin and copper occurrence in the Tremayne area of St Columb Major

46 Gold mineralisation at the southern margin of the Loch Doon granitoid complex, south-west Scotland

47 An airborne geophysical survey of the Whin Sill between Haltwhistle and Scots' Gap, south Northumberland

48 Mineral investigations near Bodmin, Cornwall. Part 3 The Mulberry and Wheal Prosper area

49 Seismic and gravity surveys over the concealed granite ridge at Bosworgy, Cornwall

50 Geochemical drainage survey of central Argyll, Scotland

51 A reconnaissance geochemical survey of Anglesey

52 Miscellaneous investigations on mineralisation in sedimentary rocks

53 Investigation of polymetallic mineralisation in Lower devonian volcanics near Alva, central Scotland

54 Copper mineralisation near Middleton Tyas, North Yorkshire

55 Mineral exploration in the area of the Fore Burn igneous complex, south-western Scotland

56 Geophysical and geochemical investigations over the Long Rake, Haddon Fields, Derbyshire

The Institute of Geological Sciences was formed by the incorporation of the Geological Survey of Great Britain and the Geological Museum with Overseas Geological Surveys and is a constituent body of the Natural Environment Research Council

Bibliographical reference
Brown, M. J. and Ogilvy, R. D. 1982. Geophysical and geochemical investigations over the Long Rake, Haddon Fields, Derbyshire. *Mineral Reconnaissance Programme Rep. Inst. Geol. Sci.*, No. 56

Photocopied in England for the Institute of Geological Sciences by Imediaprint

CONTENTS

FIGURES

TABLES

SUMMARY

Geophysical and geochemical investigations were undertaken over the Long Rake at Haddon Fields, Derbyshire in order to establish methods, or combinations of methods, showing the best response to the mineralisation. The mineralised structure carries high concentrations of fluorite with associated lead and zinc minerals and the gangue minerals baryte and calcite. The ground examined was relatively undisturbed with good geological control from drill hole data.

Gravity and magnetic anomalies such as those obtained over the Long Rake could have limited applications for the indirect location of veins the approximate position of which is known. Induced polarisation, resistivity and electro-magnetic measurements failed to produce anomalies which could be directly attributed to the mineralisation or its host structure. However, reconnaissance mapping with very low frequency electro-magnetic (VLF-EM) and Radiohm methods showed that, over a large section of the survey area, the fluor-spar vein could be mapped by its association with the subdrift shale/limestone contact.

The determination of a wide range of elements in soils and tills showed that the more mobile elements such as F and Zn are particularly useful in detecting mineralisation over broad areas. Less mobile elements tend to exhibit localised disperson patterns which have applications in precisely locating an orebody.

Elements enriched in soil above the Long Rake, in areas of thin overburden, include Pb, Ba, Sr, Ca, Zn, Rb and Th. Thickening cover towards the west tends to mask anomalies of many elements above the Rake, only Ba, Sr and Pb maintaining significant contrast.

The collection of basal till samples was made difficult by the occurrence of large limestone boulders. However, results indicated that the method has no advantage over soil geochemistry in this environment, as geochemical contrast is not improved. Levels of Ba and Ca were highly variable and the concentration of Ba appeared to be directly related to the sampling depth.

INTRODUCTION

LOCATION AND DETAILS OF THE SURVEY

The area of Haddon Fields lies on the eastern flank of the Derbyshire Dome (Figure 1) approximately 2 miles south of Bakewell between Youlgreave and Haddon Hall. It falls within the Ordnance Survey 1:50 000 Buxton, Matlock and Dovedale (119) Sheet and the Buxton (111) Sheet of the 1:50 000 geological map of England and Wales.

A strike length of 2.6 km of the Long Rake was examined, over which a total of 336 soils and 112 till samples were collected. 101 samples of drill core were analysed from material supplied by Dresser Minerals, International Inc. UK. (Analytical data are available for examination on open-file at the Institute's Keyworth office.) The survey was extended to a maximum of 220 m north and south of the Long Rake. Induced Polarisation (IP), resistivity, electro-magnetic (EM), gravity and magnetic measurements were made on selected traverses. A more detailed VLF-EM and Radiohm survey was undertaken on a 1600 m X 500 m gridded area covering a major part of the prospect. A gamma spectrometry survey was also undertaken (Brown and Ball, 1979) over the area but was only successful in mapping the higher uranium contents of the black shales and, in particular, the radioactive *Cravenoceras leion* marine band.

AIMS OF THE SURVEY

Standard geochemical and geophysical techniques may not prove successful in locating new ore deposits in areas where there is widespread contamination from previous mining activity or where the deposits lie beneath thick glacial over-burden. The aim of the survey was to define the geochemical and geophysical response of the Long Rake orebody beneath drift and shale cover in order to produce exploration criteria for the search for similar deposits. Good geological control was provided at Haddon Fields by drill core data kindly provided by Dresser Minerals, who at the time of the survey were undertaking a detailed drilling programme along the strike of the vein.

A series of different geophysical methods was used in order to identify the most useful in detecting the mineralisation at depth. The determination of a wide range of elements in soils and tills was undertaken in order to examine dispersion patterns in the overburden related to the mineralisation and to identify possible pathfinders. The possible advantages of deep till sampling over soil sampling were also investigated.

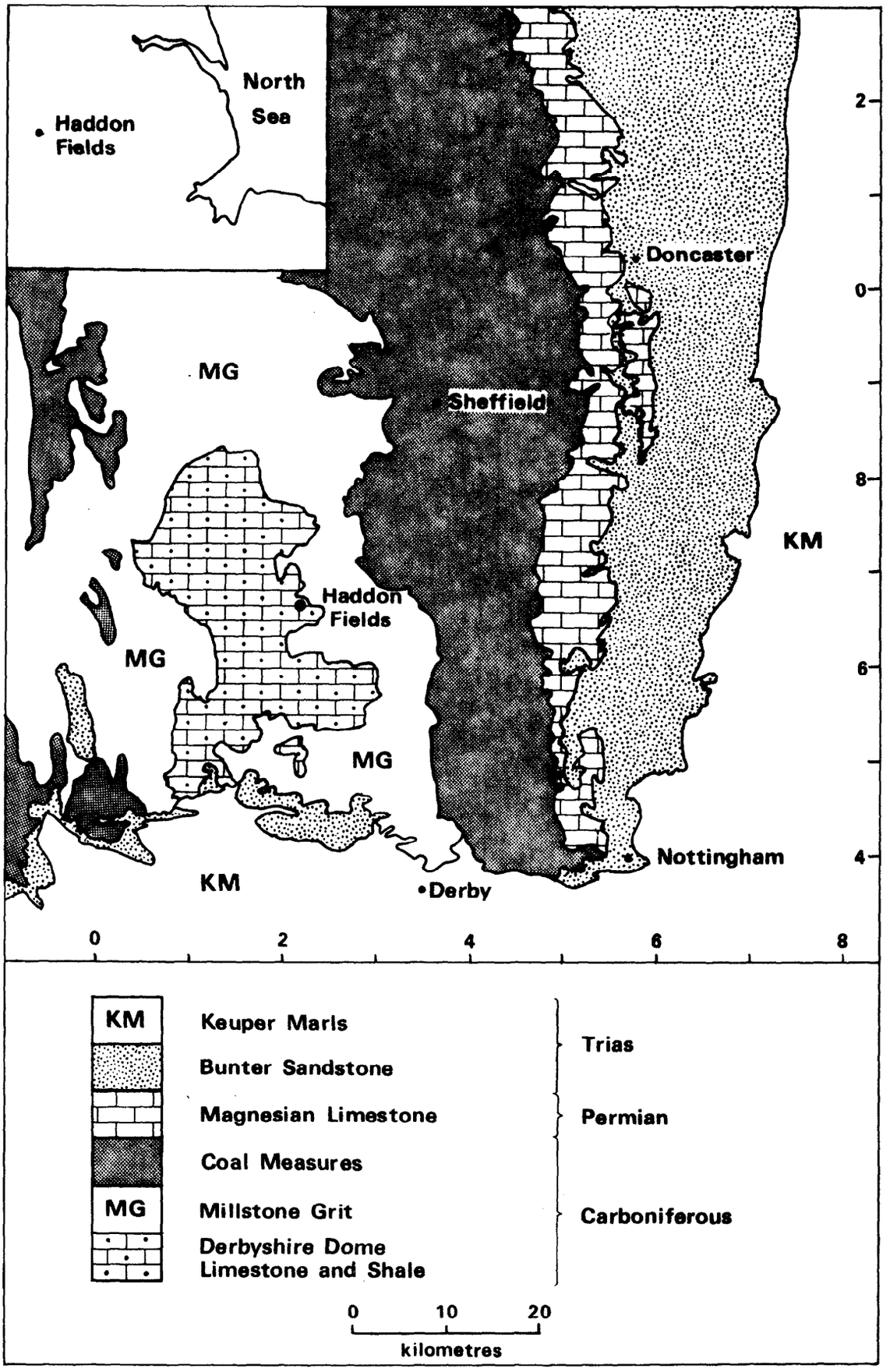

Figure 1 Location of the Survey area

GEOLOGY AND MINERALISATION

The regional geology, covering parts of the South Pennine Orefield, is fully described by Smith and others (1967) and Stevenson and Gaunt (1971). Accounts of the mineralisation and the future potential of fluorspar mining are documented by Varvill (1959), Ford and Ineson (1971) and Mason (1973).

The Long Rake is emplaced along an east-west steeply dipping to vertical fault which is cut by minor north-west trending rakes (mineralised faults). At Haddon Fields the Eyam Limestones to the north are faulted against downthrown shales of Millstone Grit age. Geological boundaries are shown on the detailed map of the area (Figure 2) based on recent revision of the 1:10 000 geological map, sheet SK 26 NW. Layers of basaltic lava and tuff, locally known as 'toadstone', are interleaved with the limestones forming an important control over the mineralisation and over the pattern of drainage. The Long Rake, which is typical of the Derbyshire style of mineralisation, carries high concentrations of fluorite with associated lead and zinc minerals, baryte and calcite. The orebody is variably covered, in the Haddon Fields area, by up to 40 m of mudstone and up to 9 m of glacial till. Within the South Pennine Orefield a zonation of both the ore and the major gangue minerals has been recognised (Schnellmann and Wilson, 1947; Dunham, 1952; Firman and Bagshaw, 1974) with fluorite being more common towards the eastern edge of the orefield and baryte and calcite to the west. Evidence from mine workings suggests an additional depth zonation, with fluorite and galena giving way to calcite and sphalerite (Smith and others, 1967).

Freezing studies of primary fluid inclusions (Rogers, 1977) from fluorite within the South Pennine Orefield indicated that the ore-forming solutions were fairly high-temperature potassic brines. It is unlikely that the Derbyshire mineralisation is directly associated with igneous activity, as the high salinities and low K/Na ratios obtained suggest that the fluids were similar to formation-waters in deep sedimentary basins (Sawkins, 1968). It has been proposed that a source area for some of the brines is the Edale and Widmerpool gulf area, with a possible contribution from the Cheshire Basin in the west (Robinson and Ineson, 1979).

Wheels Rake, a north-west trending vein cross-cutting Long Rake (Figure 2) was dated using model lead ages at 220 ± 70 Ma (Moorbath, 1962). The age of mineralisation within the South Pennine Orefield is estimated as being between Upper Permian and late Triassic (230–180 Ma, Ford, 1967). Recent K/Ar data from clays and lavas suggests dates for the mineralisation between 270 ± 7 Ma and 235 ± 5 Ma with some activity occurring up to 180 ± 2 Ma (Ineson and Mitchell, 1972).

A lithological log of a typical borehole within the survey area is shown in Appendix 3 (geology after N. Butcher, Dresser Mineals) including a gamma log showing, in particular, the response of the uraniferous marine band. After correction for the 50° inclination of the borehole the depth to the base of the shale is 28 m and to the top of the toadstone is 46 m. A tabulated description of drill core material collected from 3 boreholes drilled by Dresser Minerals along the Long Rake is included in Appendix 4.

GEOPHYSICAL INVESTIGATIONS

INTRODUCTION

Gravity measurements were made on traverses 800 W, 1400 W, 1800 W and 2830 W, (Figure 3) using a LaCoste and Romberg gravimeter. Station intervals ranged from 20 m over country rock to 5 m over the mineral vein. All measurements were tied to the NGRN 73 (National Gravity Reference Net, Masson Smith and others, 1974) using the primary gravity base station at Matlock.

Total field intensity magnetic measurements were made on the same traverses, at similar intervals, using an ELSEC proton precession magnetometer.

IP/resistivity constant separation profiling was carried out on lines 400 W, 1400 W, 1800 W and 2830 W, using a HUNTEC LOPO transmitter coupled to a HUNTEC Mk III receiver. Measurements of chargeability were obtained for a delay time of 240 ms and an integration time of 60 ms. A Schlumberger electrode configuration was used with AB/2 spacings of 10 m, 20 m or 60 m; the AB/2 spacings being selected on the basis of known geology and vertical electrical soundings (VES). The Schlumberger array was chosen for its sensitivity to thin conductive or resistive veins (Kumar, 1973). Non-polarising electrodes were used for both current and potential circuits.

Slingram EM measurements were made on traverses 400 W, 800 W, 1400 W, 1800 W and 2830 W, using an ABEM Demigun unit. Measurements were made for frequencies, 2640 Hz and 880 Hz, with horizontal co-planar coils, and separations of 60 m and 120 m. Although fluorite is a high resistivity mineral, a fluorspar vein associated with a water-saturated fault zone may appear as a conductive target (Coney and Myers, 1977).

VLF-EM measurements were made on all traverses, using a GEONICS EM16 receiver tuned to GBR (Rugby, 16.0 KHz) and NAA (Cutler, Maine, 17.8 KHz). Two source stations were used to provide optimum coupling with linear targets striking east and south-east. In conjuction with the NAA VLF survey, Radiohm measurements were made using the GEONICS EM16R resistivity attachment. Little additional effort is

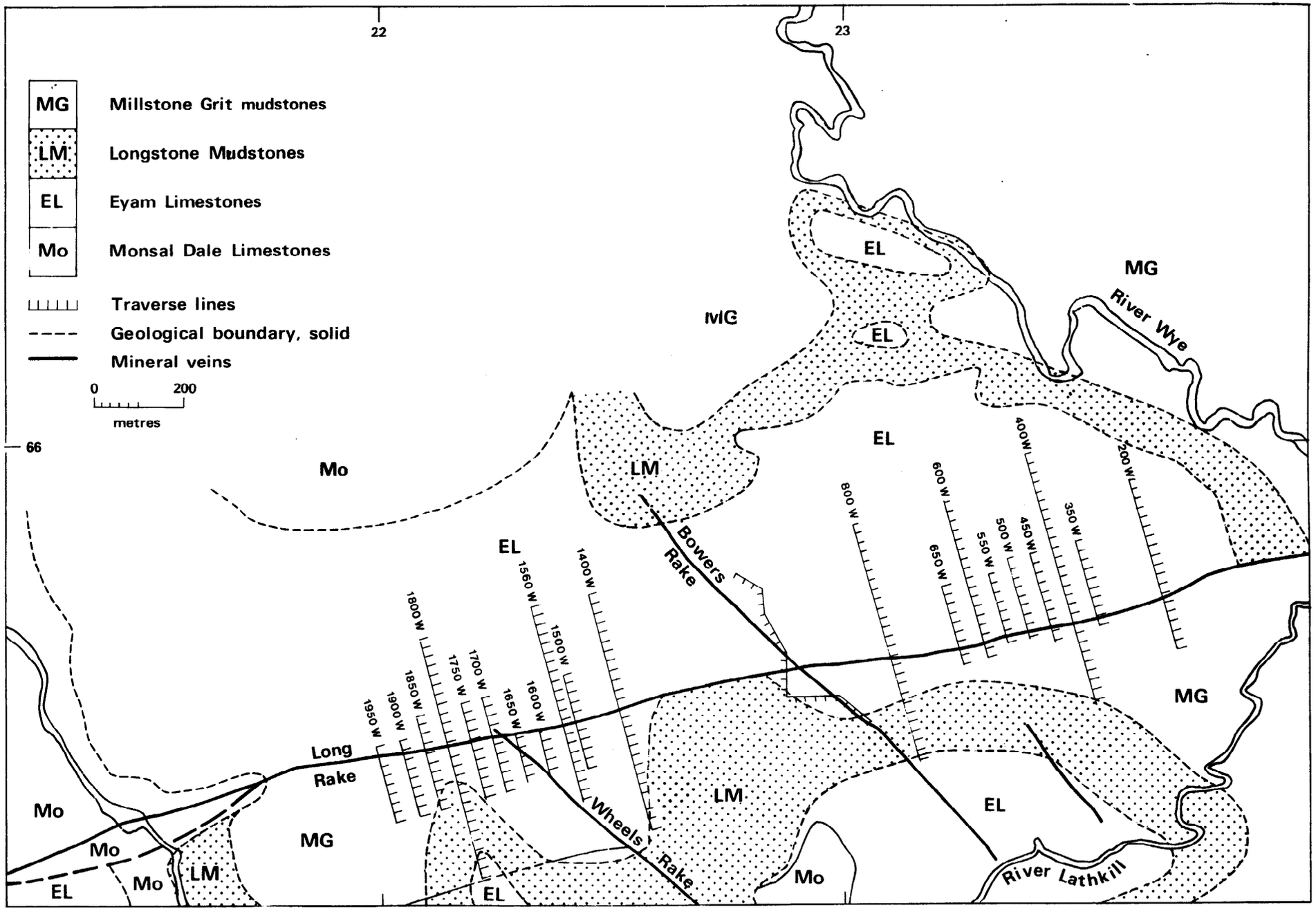

Figure 2 Surface geology and position of geochemical traverse lines

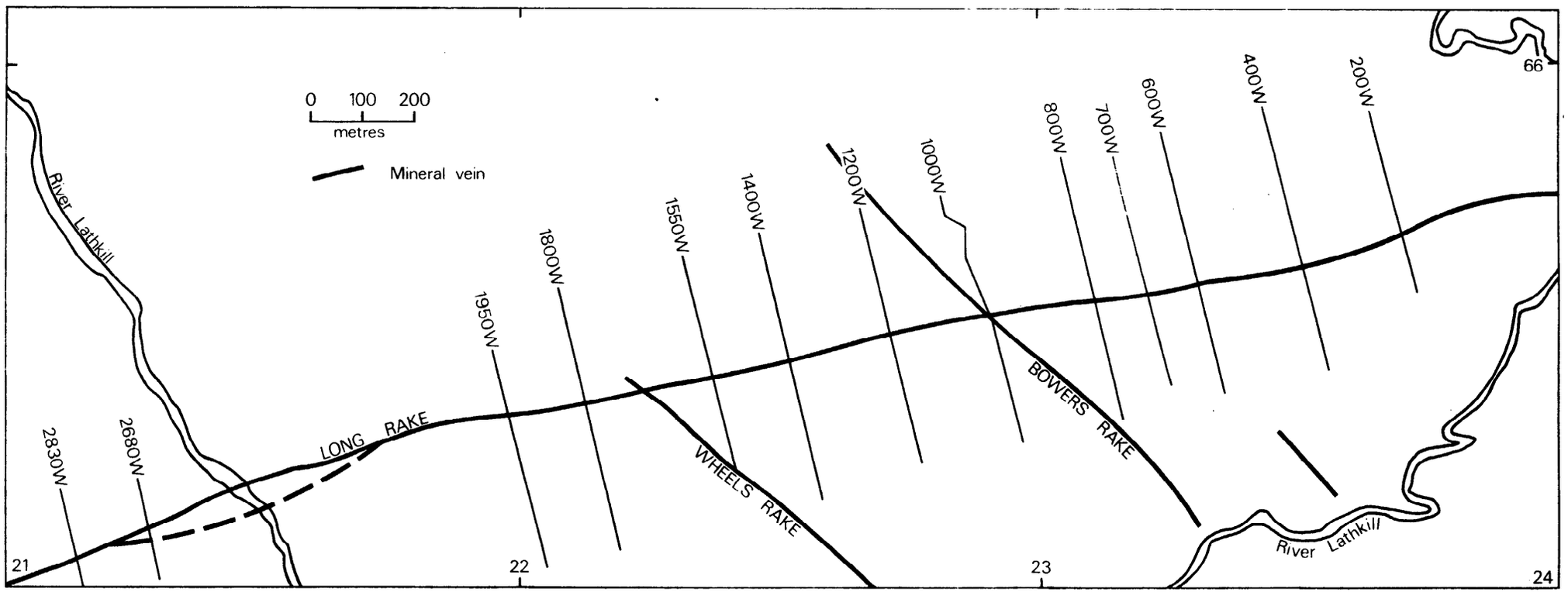

FIG. 3. LOCATION OF GEOPHYSICAL SURVEY LINES

Table 1 Rock property measurements

Drillhole No.	Depth (m)	Geological description	Magnetic susceptibility K X 10^6 (SI)	Mean saturated density (g cm^{-3})	Electrical resistivity (ohm-m)
HF 4	41	Fluorspar	13	2.92	11–26
HF 1	42	White limestone	13	2.63	3250
HF 1	52.7	White limestone	13	2.60	540
HF 1	12.1	Dark limestone	13	2.68	90
HF 3	25	Dark limestone	13	2.66	510
HF 4	24.8	Dark limestone	13	2.58	107
HF 7	25	Black shale	13	2.46	31
CF 5	52	Toadstone	17605–39485	2.76	719–1022

required in making these measurements and the potential applications of the method had not been fully assessed in this environment.

VES were made at 400 W/100 S, 1400 W/160 S, 1800 W/260 N, 1800 W/140 S and 2830 W/40 N using a Schlumberger electrode configuration. The VES were carried out to provide depth control for profiling, to determine the true resistivities of the different lithologies, and to assess the applications of VES for mapping bedrock topography and drift thickness, since the depth to bedrock could have important implications in assessing the economic potential of a fluorspar vein extending under thick cover.

Only selected results are discussed in this report but complete survey data are held on open file in the Applied Geophysics Unit of IGS, Keyworth.

PHYSICAL PROPERTY MEASUREMENTS

Rock property determinations were made on selected core samples from the Dresser Minerals drilling programme and the results are shown in Table 1.

The fluorspar shows a comparatively low mean density of 2.92 gm cm^{-3} and only a slight density contrast with the limestone.

There is a strong magnetic susceptibility contrast between the toadstone and associated rock types.

Although fluorite is a high resistivity mineral, the fluorite specimens show an anomalously low resistivity (11–26 ohm-m) compared with the limestone country rock. This difference may be explained by the brecciation of the fluorspar mineralisation, which results in a higher porosity and better conditions for electrolytic conduction.

The black shale is moderately conductive with a resistivity of 31 ohm-m.

VES RESULTS

The VES results for the survey area are shown in Figure 4, together with interpreted geo-electric sections.

Interpreted layer resistivities agreed well with laboratory observations, and the results indicated that, in most cases, adequate resistivity contrasts could be expected between the major lithological facies to permit the routine application of resistivity mapping techniques.

Borehole control confirmed that reliable estimates could be obtained on drift thickness, depth to bedrock, and in limiting cases, the depth to toadstone.

TEST TRAVERSES

For orientation purposes, geophysical measurements were initially confined to traverses 800 W and 2830 W. These cross two well defined and characteristic fluorite bodies. The results are shown in Figures 5 and 6.

On both traverses, a minor Bouguer anomaly low of 0.15–0.2 mgals was obtained over the mineralised zone. It appears that the higher density of fluorite is more than compensated by the mass deficiency caused by cavities or voids in the fault structure. In the hope that larger, more massive, fluorite bodies might be located, additional gravity observations were made on lines 400 W, 1400 W and 1800 W. The results, not shown in this report, gave similar Bouguer anomaly troughs over the fault.

The magnetic profile on 800 W shows a fairly broad, low-amplitude anomaly of 60 nT. The response is characteristic of a 'step type' structure and, on physical property evidence, is almost certainly related to the faulted toadstone. However, theoretical modelling assuming induced magnetisation and a step model compatible with the known geometry of the toadstone, could not be reconciled with the observed data. A similar result was obtained for the anomaly on 2830 W and suggests that remanent magnetisation may assume a more significant role than induced magnetisation. It seems possible that refined quantitative interpretations could provide useful structural information but this would first necessitate a more comprehensive testing of laboratory samples to determine the relative strength and direction of the

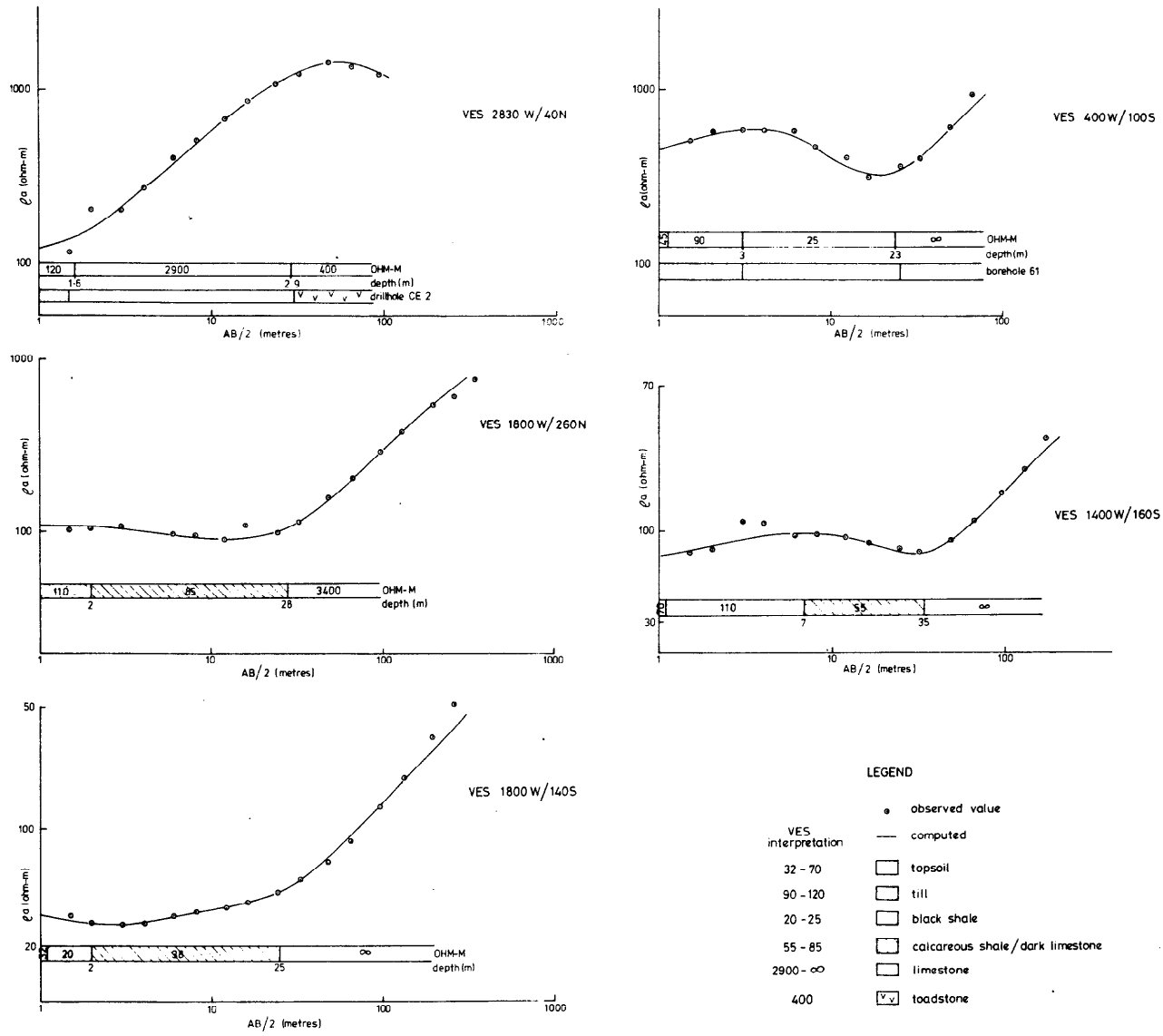

FIG. 4 . VERTICAL ELECTRICAL SOUNDING RESULTS

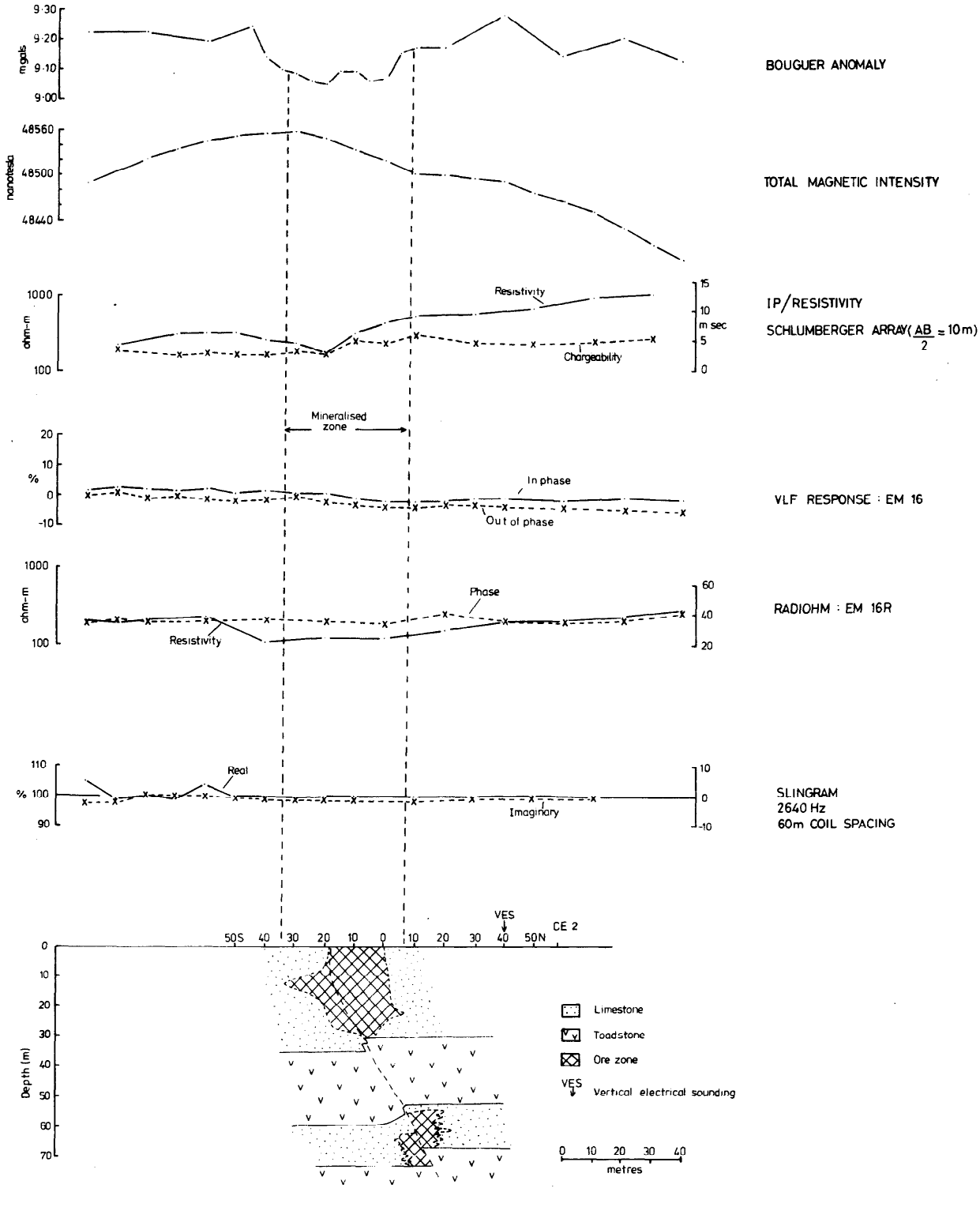

FIG. 5. GRAVITY, MAGNETIC, IP/RESISTIVITY, VLF EM, RADIOHM AND SLINGRAM RESULTS, LINE 2830 W

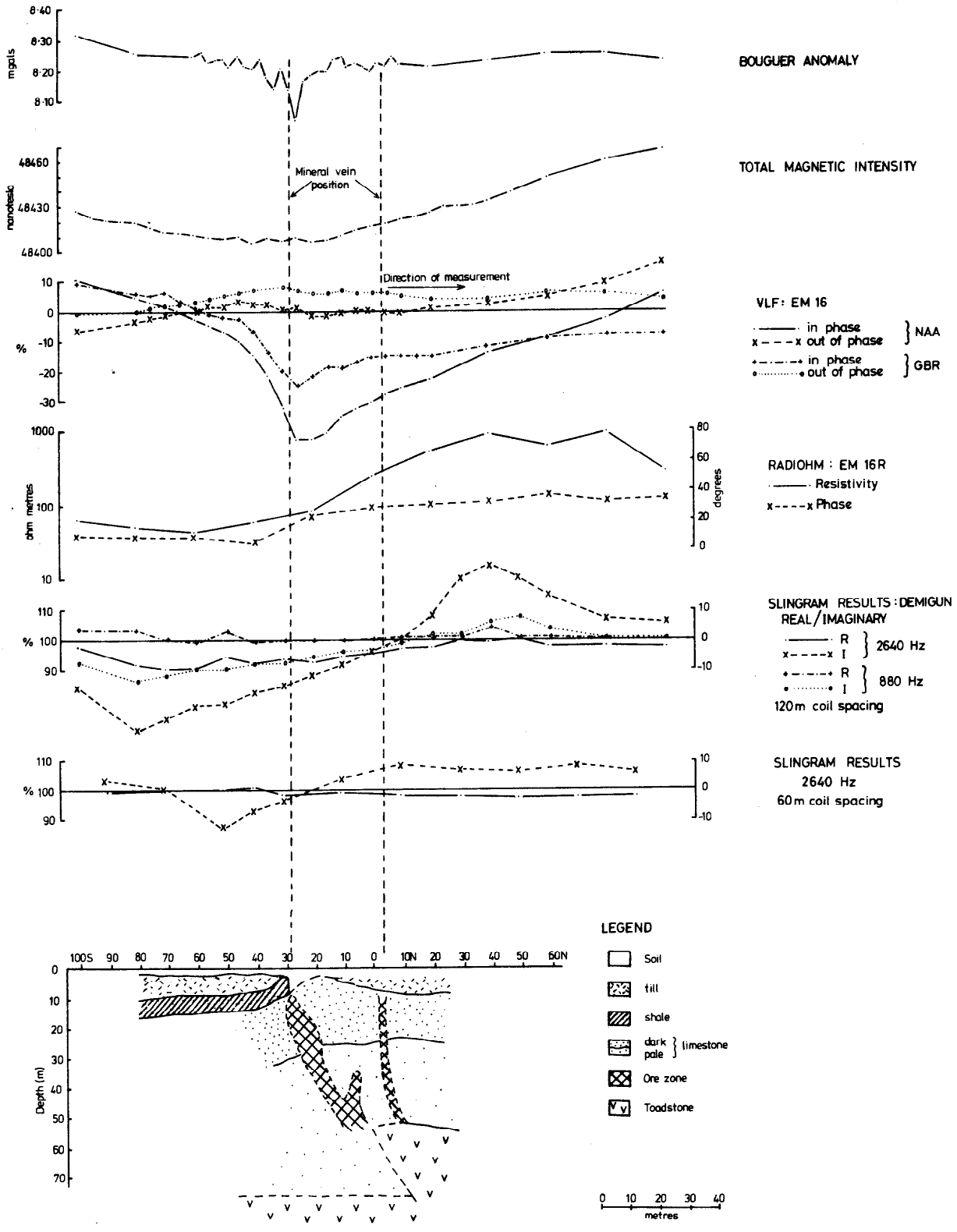

FIG. 6. GRAVITY, MAGNETIC, VLF EM, RADIOHM AND SLINGRAM RESULTS. LINE 800 W

remanent component.

On Traverse 2830 W, the IP/resistivity, Slingram EM, VLF-EM and Radiohm profiles are practically featureless, indicating that there is no discernible geoelectric contrast between the mineralised zone and the host rock. The absence of an anomalous IP response reduces the possibility of any significant sulphide mineralisation being present. Negligible IP responses were also obtained on 400 W, 1400 W and 1800 W.

On traverse 800 W, the juxtaposition of the shale and limestone lithologies at the fault boundary produced significant conductivity anomalies, coincident with the known position of the vein. With NAA, a strong VLF-EM in-phase anomaly, exceeding 50%, was recorded above the shale/limestone contact. It may be noted that the edge of the shale occurs beneath the steepest profile gradient (i.e. at 80 S) and not at the nominal cross-over point on the zero line. A similar but less pronounced anomaly was obtained with GBR, indicating that the causative source has a favourable strike direction for both stations. This would not have been the case for a narrow east-west striking fault zone.

This observation was confirmed by the Slingram EM survey. The near horizontal attitude of the conductor is reflected by the southerly displacement of the negative peak response, on increasing the coil separation from 60 m to 120 m. There is no indication that the shale is masking the response of a conductive fault zone dipping steeply to the north. The poor quality of the conductor is demonstrated by the dominant response of the imaginary component, and the marked increase in both components, on increasing the excitation frequency from 880 Hz to 2640 Hz. This discriminatory response is in contrast to the VLF-EM results, where the high frequency places the response parameter of the shale beyond the range where appreciable quadrature effects are generated.

The Radiohm profiles on 800 W show a low apparent resistivity (40 ohm-m) over the shale, increasing to 200 ohm-m over the limestone. The phase values are lower than 45° on both sides of the fault, indicating a multilayer earth, and increasing resistivity with depth. To the north of this profile section, true resistivity values of 600–1000 ohm-m were obtained over sub-outcropping limestone.

Similar resistivity and EM results were obtained over the subdrift shale/limestone contact on traverses 400 W, 1400 W and 1800 W. Contrary to expectations, and physical property evidence, it would appear that, in situ, there is little or no preferential electrolytic conduction along the fault zone, and the fluorspar vein does not appear as a conductive feature.

VLF-EM RESULTS

To assist delineation of the fluorspar vein by its association with the shale/limestone contact, contour maps of the filtered in-phase component values were prepared (Fraser, 1969).

Examination of the NAA contour map (Figure 7) shows a major east-west trending anomaly (A) extending from 200 W to 1950 W. The zero contour line corresponds well with the mapped position of the fluorspar vein. Between 1200 W and 1500 W the anomaly is less pronounced and this may reflect the presence of a more resistive transition lithology (e.g. calcareous shale or dark limestone) and/or a thickening of the overburden. There is evidence from VES and Radiohm resistivity data that both effects may be important.

A second collinear anomaly (B) of smaller amplitude occurs to the north. This anomaly is not associated with any obvious topographic or surface phenomena and drillhole evidence precludes a shale horizon. The anomaly most probably reflects a shallow conductivity contrast with a bedrock trough, or irregularities in the overburden.

The filtered in-phase values for GBR are shown in Figure 8. Owing to the two-dimensional nature of the conductive horizons, the essential features of the NAA contour pattern are retained, but the correlation of anomaly (A) with the fluorspar vein is less obvious. The major east-west trending anomalies appear to be rotated clockwise, giving an east-south-east strike direction. This distortion is attributed to the preferential enhancement of linear north-south striking features at the expense of east-west features. In particular, anomaly (C), which is well developed for GBR, is barely evident for the NAA station. Separating out effects of this kind justifies the use of two transmitter stations located in orthogonal directions, and illustrates the importance of optimum coupling with the desired target.

RADIOHM RESULTS

Histograms of apparent resistivity and phase values are shown in Figure 9.

Phase values are predominantly below 45°, indicating a multilayer earth, and increasing resistivity with depth, over most of the survey area. The resistivity values show a tri-modal distribution with peaks at 12.6 ohm-m, 79.4 ohm-m and 199 ohm-m. Caution is required in making a statistical assessment of the apparent resistivity data, due to the dependency of apparent resistivity on skin depth and layer sequence. This interdependence is illustrated in Appendix 1 where apparent resistivity and phase values are plotted for increases in thickness ratio of the top two layers for two typical geo-electric sections. It will be noted that relatively thin conductive surface layers may significantly depress the apparent resistivity values obtained over limestone bedrock. However, the distribution in Figure

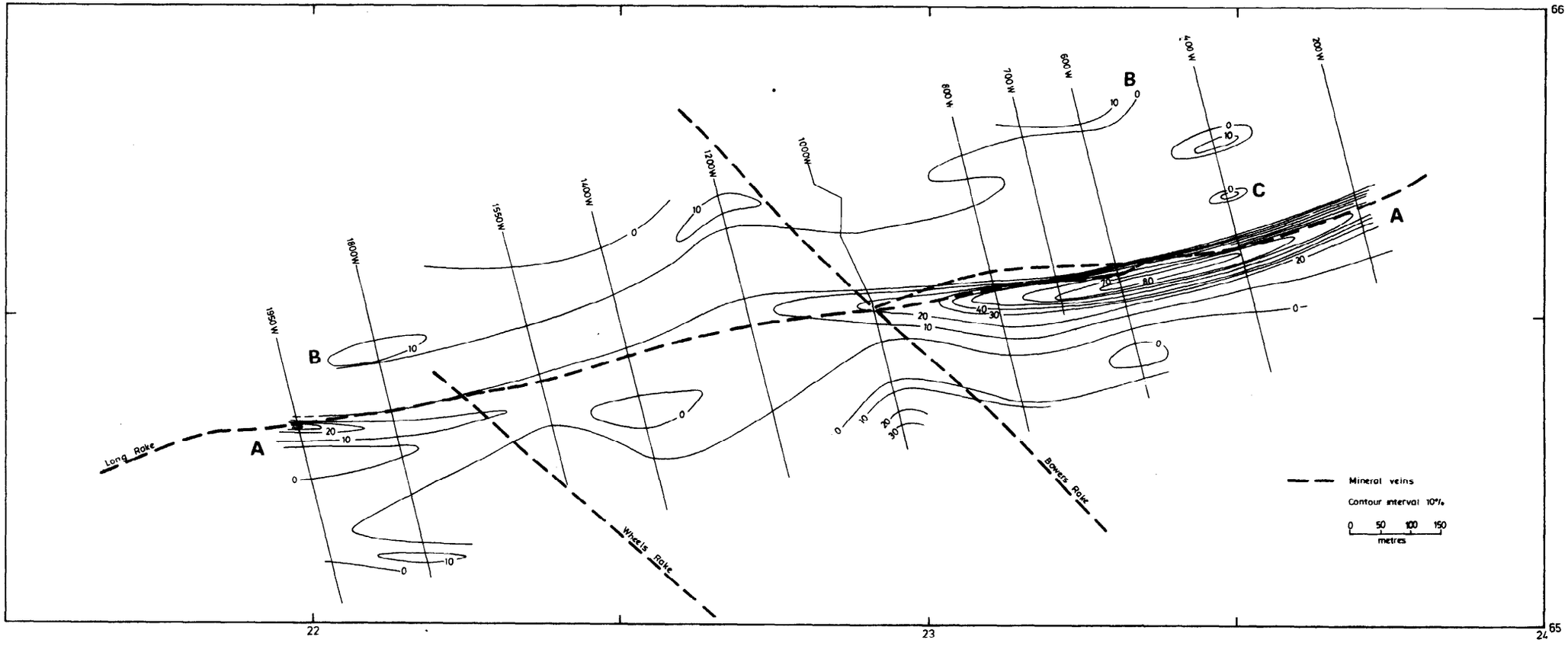

FIG. 7. CONTOURED MAP OF FILTERED VLF EM VALUES (NAA)

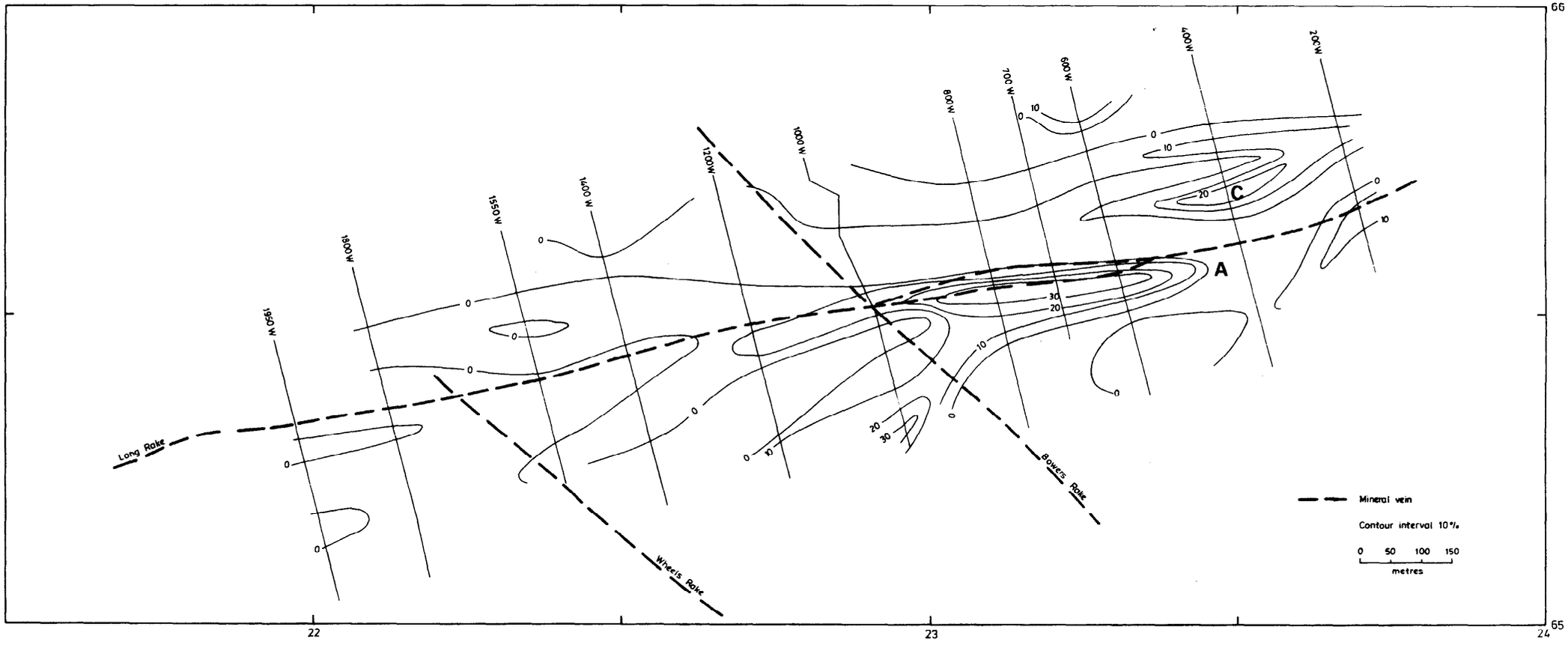

FIG. 8. CONTOURED MAP OF FILTERED VLF EM VALUES (GBR)

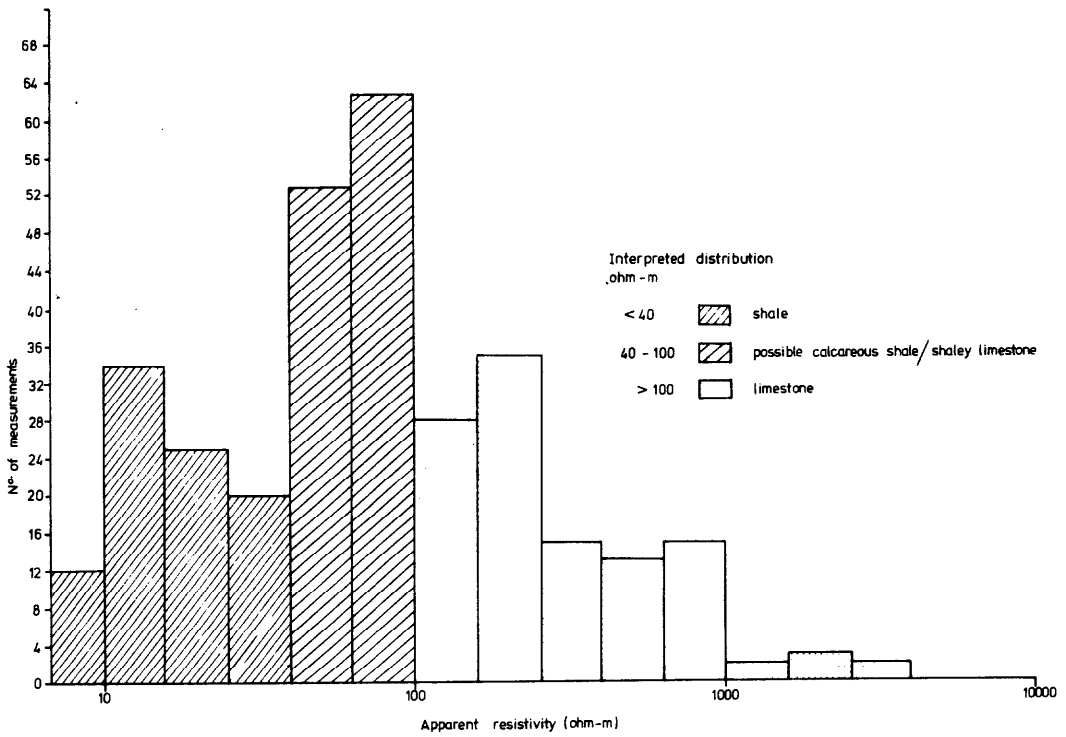

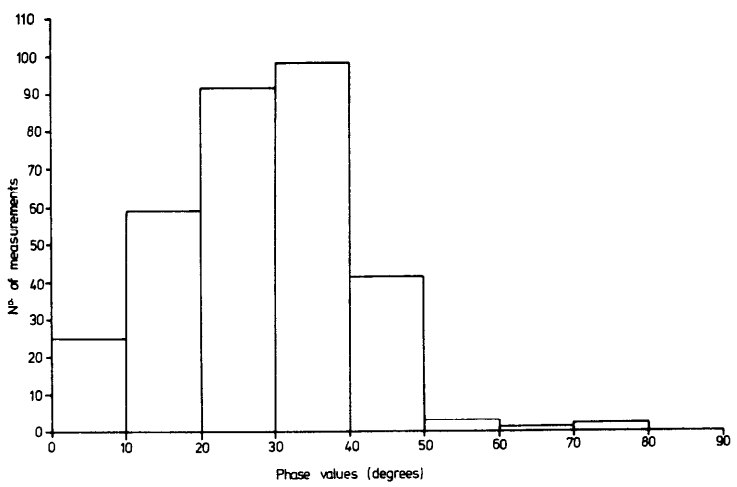

FIG. 9 HISTOGRAMS OF RADIOHM RESISTIVITY AND PHASE VALUES

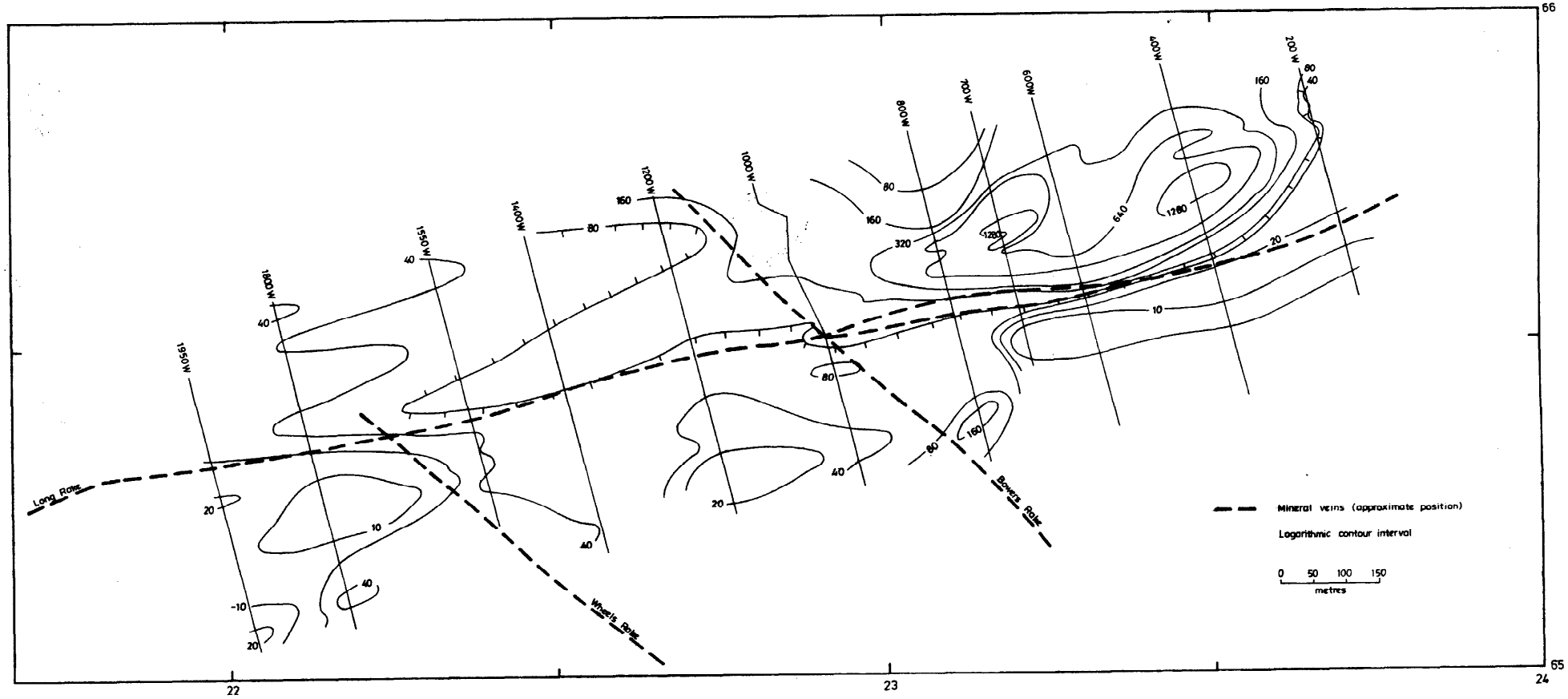

FIG. 10 CONTOURED MAP OF RADIOHM RESISTIVITY VALUES

8 is not inconsistent with the range of true resistivities obtained for the three dominant lithologies, by laboratory measurements and electrical sounding. On this basis, resistivity values less than 40 ohm-m are attributed to shale and greater than 100 ohm-m to limestone. Resistivity values of 40–100 ohm-m could be indicative of shaley limestone but some ambiguity exists in this range, due to the inability to separate geometrical effects from geological variations.

The Radiohm resistivities are shown in contour form in Figure 10. Two features are evident; a zone of high resistivities (>80 ohm-m) to the north and east, and a zone of moderate to low resistivities to the south and west. The zone of high resistivity also certainly reflects the presence of near-surface resistive limestone, and the zones of less than 40 ohm-m would suggest the presence of shale bedrock. Zones of 40–100 ohm-m are not assigned to any particular rock type, due to the ambiguity mentioned. It may be noted, however, that the resistivity gradient delineated by the 80 ohm-m contour between 400 W, 1550 W corresponds moderately well with the contact boundary defined by VLF-EM and the approximate position of the vein.

Attempts to obtain the bedrock from the fixed frequency Radiohm data were in most cases unsuccessful, due presumably to the presence of a multilayer sequence. Despite this, it would appear that alternative EM sounding methods could offer a number of operational and interpretational advantages over DC methods. There are logistic difficulties with conventional VES, in laying out long lines in areas which are intensively farmed. A further advantage of EM sounding would be the smaller sampling area, permitting local variations in drift thickness to be mapped.

GEOCHEMICAL INVESTIGATIONS

INTRODUCTION

Soil samples and profiled till samples were collected over an area of high ground between Lines 200 W and 1950 W (Figure 2) with an elevation range between 125 m and 188 m.

A total of 336 soil samples were collected, using a hand auger, at intervals of 20 m along 21 traverse lines normal to the Long Rake; from B–horizon material where developed, from 30–80 cm below surface. Profiled and deep till samples were collected using a 'Minuteman' mechanical auger at 43 sites (Figure 11) in the manner described by Smith and Gallagher (1975). Where possible a basal till sample was collected at the rock/till interface. Till depths varied between 0.5 m and 3.0 m, giving an average till depth of 1.57 m over the 5 lines samples (Figure 11). Hole 8 at the south end of Line A (Figure 11) penetrated 7.5 m of blue/grey varved clay.

A typical profile consists of a black silty organic-rich A–horizon from 0 to 30 cm. Below, to a depth of around 80 cm, the B–horizon consists of a brown to orange clay containing angular chert, subrounded limestone and some shale fragments. The C–horizon, best seen in deep overburden in the west, is transported glacial till made up of a grey to yellow clay, sometimes water saturated, with bands of chert and fragments of chert, limestone and shale of varying size.

Determinations made on a series of soil samples from the area showed a range in pH between 4.8 and 7.1 with an average of pH 6.0.

Soil and till samples were dried, crushed in a mortar and sieved to 80 mesh (BSI), and a 12 g split was taken for grinding with elvacite binder for XRF analysis. Elements determined by XRF were Ca, Ti, Mn, Fe, Ni, Cu, Zn, As, Rb, Sr, Y, Zr, Nb, Mo, Ag, Sn, Sb, Ba, Ce, Pb, Th and U. F was determined by specific ion electrode (Ficklin, 1970), after total extraction using a Na_2CO_3/KNO_3 fusion mixture follwed by dissolution in de-ionised water and addition of a suitable buffer to adjust the pH.

All the elements determined, with the exception of Sn, Ag, Fe, Mn, Ti, Nb, Zr and F which showed no distinct anomaly pattern, are plotted on single element maps, based on class intervals, which are included in Appendix 2.

Previous geochemical sampling over the Long Rake was undertaken by Farrell (1974) who concluded that anomalous levels of F, Zn and Pb in transported till should be treated with caution as they appear to vary in intensity depending on the depth of overburden, although F could be used with good success as a direct indicator of mineralisation in areas of residual soil. The Long Rake in the vicinity of Haddon Fields, and the line of the assumed sub-outcrop of the fault beneath Namurian cover, were examined using soil geochemistry by Al-Kufaishi (1969). It was concluded that trace element anomalies marked the line of the Rake and showed it to continue, with a marked displacement to the south, in an easterly direction through Little Rowsley [SK 260 659].

DATA INTERPRETATION

Summary statistics throughout the text give the geometric mean (the antilog of the mean of $\log_{10}$ transformed data), as most elements tended towards a lognormal distribution as shown by the cumulative frequency diagrams (not illustrated).

Cumulative frequency diagrams were constructed for each element using the method described by Lepeltier (1969); and class intervals were derived from the break in slope of the curve and used in the preparation of the maps in Appendix 2. Where breaks in slope could not be identified, the anomalous population was taken to include those values above the 97.5 percentile.

Elements determined in the deep till samples were plotted graphically (Figure 12) along the

traverse lines to give visual recognition of high values and also to illustrate the different levels of each element compared to the corresponding sub-surface soil from the same profile (Figure 13).

DISPERSION OF ELEMENTS IN SOIL

Maps showing the dispersion of single elements are shown in Appendix 2 to supplement the following text. Summary statistics for the soil data are given in Table 2 and a matrix of correlation coefficients in Table 3.

Anomalous patterns of certain groups of elements in soil can be attributed to (a) mineralisation, (b) the areas of underlying black shale and (c) the uraniferous marine band identified by the presence of *Cravenoceras leion.*

Anomalous patterns of Ba, Pb, Ca and Sr (see maps Appendix 2) provide surface evidence of the existence of the east-west trending Long Rake and the associated north-west trending Bowers and Wheels Rakes. High levels of F and Zn are directly related to the mineralisation, although due to a wide dispersion pattern they tend to give high background levels over the area surveyed. Rb and Th are clearly related to the Long Rake in the east although no anomalous patterns can be identified in the west.

High levels of Ba (>0.40%) are dispersed up to 60 m from the mapped line of the Rake in the east and levels over 0.1% are found 240 m north and south of the Rake in the west. The Ba anomalies in the east, where the overburden is relatively shallow, are closely confined to the strike of the Long Rake.

Pb anomalies (>0.50%) clearly identify the Rake in the east and correlate very closely with Ba anomalies; but these fail to give a clear pattern in the west. Both Zn and Th show a significant positive correlation with Pb (Table 3) and show similar dispersion patterns, particularly in the east of the area. Although contamination due to material from old trial pits would give rise to false Pb anomalies they were easily identified in the field and, therefore, omitted on soil traverse lines.

Ca shows high levels in soil (>2.0%), following the line of the Rake in the east most probably due to a high proportion of fluorite within the soil above the vein. A clear dispersion pattern is not present in the west, the higher values being randomly distributed (Appendix 2).

Sr, which exhibits a significant positive correlation with Ba, and to a lesser extent with Pb (Table 3), gives a direct indication of the mineralisation. Sr^{2+} has an ionic radius between Ca^{2+} and Ba^{2+}, hence it tends to behave in a similar manner although it is less mobile than Ca under weathering conditions.

Because of its high solubility over a wide pH range, F produces high background levels and a wide dispersion pattern over the whole of the area surveyed. The main advantage of using F in soils as an indicator of mineralisation is the availability of a quick, precise method of analysis, using a specific ion electrode (Ficklin, 1970), which can be applied in a field laboratory. Determinations can be made after cold partial extraction, or total extraction, of F^- and the addition of a suitable buffer to adjust the pH and release any F^- complexed with polyvalent cations such as Al^{3+} and Fe^{3+}.

Zn shows high background levels ($\bar{x}$ = 460 ppm) over the entire survey area. Worldwide averages for Zn in soil are 50 ppm (Vinogradov, 1959) and 75 ppm for North American basal till samples (Beyrock and Pawluk, 1967). The concentration of Zn in the weathering regime is controlled more by adsorption than by solubility. Zn is leached under oxidising conditions and adsorbed onto Fe and Mn oxides in addition to clay minerals and organic material. The dispersion pattern of Zn in the east clearly follows that of Ba, Pb and Ca along the strike of the Rake but no anomalous dispersion occurs to the west.

Rb anomalies in soil are associated with a varved clay deposit overlying the Longstone Mudstone in the west but there are no anomalies

Table 2 Summary statistics for soil samples

	Hand auger samples	
Element	Soils n = 336	
	$\bar{x}\ \log_{10}$	σ
F	795*	—
Ca	0.98%	0.30
Ti	6160	0.06
Mn	980	0.20
Fe	6.0%	0.05
Ni	83	0.12
Cu	54	0.13
Zn	460	0.22
As	14.5	0.16
Rb	95	0.06
Sr	93	0.16
Y	42	0.10
Zr	275	0.08
Nb	13	0.06
Mo	3	0.37
Ag	1	0.20
Sn	2	0.27
Sb	5	0.30
Ba	1200	0.37
Ce	45	0.10
Pb	980	0.31
Th	12	0.13
U	6	0.14

*Arithmetic mean

Values in ppm except where otherwise indicated

traverse lines to give visual recognition of high values and also to illustrate the different levels of each element compared to the corresponding sub-surface soil from the same profile (Figure 13).

DISPERSION OF ELEMENTS IN SOIL

Maps showing the dispersion of single elements are shown in Appendix 2 to supplement the following text. Summary statistics for the soil data are given in Table 2 and a matrix of correlation coefficients in Table 3.

Anomalous patterns of certain groups of elements in soil can be attributed to (a) mineralisation, (b) the areas of underlying black shale and (c) the uraniferous marine band identified by the presence of *Cravenoceras leion.*

Anomalous patterns of Ba, Pb, Ca and Sr (see maps Appendix 2) provide surface evidence of the existence of the east-west trending Long Rake and the associated north-west trending Bowers and Wheels Rakes. High levels of F and Zn are directly related to the mineralisation, although due to a wide dispersion pattern they tend to give high background levels over the area surveyed. Rb and Th are clearly related to the Long Rake in the east although no anomalous patterns can be identified in the west.

High levels of Ba (>0.40%) are dispersed up to 60 m from the mapped line of the Rake in the east and levels over 0.1% are found 240 m north and south of the Rake in the west. The Ba anomalies in the east, where the overburden is relatively shallow, are closely confined to the strike of the Long Rake.

Pb anomalies (>0.50%) clearly identify the Rake in the east and correlate very closely with Ba anomalies; but these fail to give a clear pattern in the west. Both Zn and Th show a significant positive correlation with Pb (Table 3) and show similar dispersion patterns, particularly in the east of the area. Although contamination due to material from old trial pits would give rise to false Pb anomalies they were easily identified in the field and, therefore, omitted on soil traverse lines.

Ca shows high levels in soil (>2.0%), following the line of the Rake in the east most probably due to a high proportion of fluorite within the soil above the vein. A clear dispersion pattern is not present in the west, the higher values being randomly distributed (Appendix 2).

Sr, which exhibits a significant positive correlation with Ba, and to a lesser extent with Pb (Table 3), gives a direct indication of the mineralisation. Sr^{2+} has an ionic radius between Ca^{2+} and Ba^{2+}, hence it tends to behave in a similar manner although it is less mobile than Ca under weathering conditions.

Because of its high solubility over a wide pH range, F produces high background levels and a wide dispersion pattern over the whole of the area surveyed. The main advantage of using F in soils as an indicator of mineralisation is the availability of a quick, precise method of analysis, using a specific ion electrode (Ficklin, 1970), which can be applied in a field laboratory. Determinations can be made after cold partial extraction, or total extraction, of F^- and the addition of a suitable buffer to adjust the pH and release any F^- complexed with polyvalent cations such as Al^{3+} and Fe^{3+}.

Zn shows high background levels ($\bar{x}$ = 460 ppm) over the entire survey area. Worldwide averages for Zn in soil are 50 ppm (Vinogradov, 1959) and 75 ppm for North American basal till samples (Beyrock and Pawluk, 1967). The concentration of Zn in the weathering regime is controlled more by adsorption than by solubility. Zn is leached under oxidising conditions and adsorbed onto Fe and Mn oxides in addition to clay minerals and organic material. The dispersion pattern of Zn in the east clearly follows that of Ba, Pb and Ca along the strike of the Rake but no anomalous dispersion occurs to the west.

Rb anomalies in soil are associated with a varved clay deposit overlying the Longstone Mudstone in the west but there are no anomalies

Table 2 Summary statistics for soil samples

Element	Hand auger samples Soils n = 336	
	$\bar{x}\ \log_{10}$	σ
F	795*	–
Ca	0.98%	0.30
Ti	6160	0.06
Mn	980	0.20
Fe	6.0%	0.05
Ni	83	0.12
Cu	54	0.13
Zn	460	0.22
As	14.5	0.16
Rb	95	0.06
Sr	93	0.16
Y	42	0.10
Zr	275	0.08
Nb	13	0.06
Mo	3	0.37
Ag	1	0.20
Sn	2	0.27
Sb	5	0.30
Ba	1200	0.37
Ce	45	0.10
Pb	980	0.31
Th	12	0.13
U	6	0.14

*Arithmetic mean

Values in ppm except where otherwise indicated

associated with the Rake in this area. However, to the east there is a significant dispersion of high Rb above the Long Rake. Other researches have shown (Al Atia and Barnes, 1976; Steed and others, 1976) Rb to be an ideal pathfinder in soils for Au and possibly Pb mineralisation.

Cu, apart from being enriched in soils overlying the black shales and the Longstone Mudstone, shows anomalous levels over the area of Wheels Rake and Bowers Rake although these may be due to contamination, particularly over Wheels Rake as high levels of Zn, As, Ba, Pb and Th are also recorded. Ni and As show significant positive correlation with Cu (Table 3) and follow similar dispersion patterns (Appendix 2). The mean for Cu over Haddon Fields ($\bar{x}$ = 54 ppm) is higher than recorded worldwide averages (20 ppm; Vinogradov, 1959). The dispersion of Cu, like Zn, is controlled to a major extent by adsorption onto Fe and Mn oxides rather than by solubility. It is mobile in the secondary environment below a pH of 5.3 but most soils in the Haddon Fields area show a higher pH level (mean pH = 6.0).

Th, normally an immobile element in the secondary environment in wet temperate areas, shows a significant positive correlation with Pb and to a lesser extent with Ba and Zn (Table 3). Anomalies appear to be associated with Bowers and Wheels Rake and with the Long Rake in the east of the area on Lines 200 W, 500 W, 600 W and 650 W.

Rb, As, Mo, Th, U and Cu are enriched in soils to the south of Line 1800 W, overlying the Longstone Mudstone, over which has developed a deposit of varved clay which is considered to be the cause of the anomaly, as a similar pattern is not present over the Longstone Mudstone on Line 800 W (Figure 2).

Relatively high levels of Ni, Cu, As, Mo and U in soils are evident in the north-east, particularly on Line 400 W. It is suggested that these anomalies are associated with the sub-outcrop of black shales, although the area is shown as limestone on the 1:10 560 geological map. High levels of U are recorded along Lines 200 W and 400 W with associated high Cu, Mo and As in soil. These anomalies are thought to be related to the sub-outcrop of the *Cravenoceras leion* marine band, which is known to be uraniferous and is easily recognised in the gamma log of borehole HF 7 (Appendix 3).

Rare earth elements Ce and Y show no distinct pattern but Ce/Y ratios give more meaningful results and can be related to the underlying geology. In general, higher Ce/Y ratios are indicative of sub-outcropping black shales whereas lower ratios are associated with underlying carbonate rocks.

Ti, Mn, Fe, Zr and Nb levels in soil show no pattern and little divergence from background over the survey area and have not been plotted in map form. Although of little use as pathfinders for mineralisation, levels of Fe and Mn are useful in

Table 3 Correlation coefficients for 298 soil samples (log-transformed data)

Element	0.7–0.8	0.6–0.7	0.5–0.6	0.4–0.5	0.3–0.4
Ca		Sr	-Zr		-Ti, -Nb
Ti				-Sr, Fe	-Ba, -Ca, Zr
Mn			Fe		Zn, Ni, As, Mo
Fe		Ni	Mn, Rb	Cu, Ti	As, Y
Ni	Cu	Fe, Y	Zn		-Zr, Mn
Cu	Ni	As	U, Y	Zn, Fe, Mo	-Zr
Zn		Pb	Ba, Ni, Th	Cu, Y	Sr, -Ce, Mn
As		Cu		Zn, U, Rb, Mo	Fe, Mn, Th, Y
Rb			Fe	Th, As	
Sr	Ba	Ca	-Ce, Ca	-Ti	Zn, Pb, Th, -Zr
Y		Ni	Cu	Zn	Fe, U, As
Zr			-Ca		Nb, Ti, -Sr, -Ni, -Cu
Nb					-Ca, Zr
Mo				Cu, U, As	Mn
Ag					
Sn			Sb		
Sb			Sn		
Ba	Sr	Pb	Zn, -Ce, Th		-Ti
Ce			-Ba, -Sr		-Pb, -Zn
Pb		Th, Ba, Zn			-Ce, Sr
Th		Pb	Ba, Zn	Rb	Sr, As
U			Cu	Mo, As	Zr

Table 4 Summary statistics for deep till samples

Element	Deep till samples n = 43	
	$\bar{x}$ $\log_{10}$	σ
Ca	5.75%	0.41
Ti	4470	0.11
Mn	850	0.18
Fe	4.68%	0.11
Ni	90	0.11
Cu	60	0.13
Zn	400	0.22
As	14	0.23
Rb	70	0.15
Sr	174	0.17
Y	40	0.14
Zr	195	0.13
Nb	12	0.08
Mo	5	0.27
Ag	1	0.36
Sn	1	0.50
Sb	1	0.54
Ba	1514	0.35
Ce	38	0.16
Pb	760	0.30
Th	8	0.13
U	6	0.19

Values in ppm except where otherwise indicated

the interpretation of data because of their ability to adsorb trace elements such as Cu and Zn. Sb, although plotted in map form exhibits no anomaly patterns.

ANOMALY PATTERNS IN SOILS

Localised dispersion patterns of Pb, Zn, Ba, Sr, Ca, Rb and Th identify clearly the location and strike of the Long Rake in the east of the area surveyed. This group of elements shows a dispersion to the north due to both downslope movement of the till and downslope hydromorphic dispersion of the more mobile elements. Physical transport of the till is indicated by the dispersion of immobile elements such as Th and Pb and may be due to a localised northerly movement of the ice.

A similar dispersion pattern is not repeated in the west of the area; only Ba and Sr anomalies identify the Rake, and these elements do not delineate it as precisely as in the east. Pb anomalies are fairly randomly distributed both north and south of the Rake in the west except on Line 1400 W where one Pb anomaly, with associated high Zn, Ba and Ca, coincides with the position of the Rake. However, due to the occurrence of a number of old pits along the Rake the anomaly could be due to contamination.

It is considered that the contrast between the anomaly patterns in the east and west of the area is directly related to a thickening of the till cover towards the west.

DISTRIBUTION OF ELEMENTS IN DEEP TILLS

Summary statistics for 43 deep till samples are shown in Table 4. Samples were collected using a power auger from five traverse lines A–E (Figure 11), normal to the Long Rake. The deepest samples from Lines D and E represent basal till. However, along Lines A, B and C it was not always possible to reach the rock/till interface because of the occurrence of large boulders of limestone within the overburden. The levels of Ca, Fe, Ba, Pb and Zn along each traverse line are represented graphically (Figure 12) and correlated with the geology.

The Ca content of the deep tills ($\bar{x}$ = 5.75%) is higher than that recorded in sub-surface soils ($\bar{x}$ = 0.98%) but shows very variable dispersion patterns both north and south of the Rake. Similarly Ba is more highly concentrated in deep tills ($\bar{x}$ = 1514 ppm) than soil ($\bar{x}$ = 1200 ppm) but again, like Ca, it gives rise to variable dispersion patterns making interpretation difficult. The only obvious Ba anomaly associated with the Long Rake is on Line C (Figure 12c) where corresponding Pb and Zn anomalies are also present. A steady increase of Ba and Pb to the south along Line C may be due to glacier transport of the basal till. Along most lines there is a correlation of Ca with Ba and little variation in Fe levels although there is a suggestion of a negative correlation with Ca and Ba along Lines A, B and C (Figure 12).

Because both Ba and Ca show variable patterns in deep tills, and because of the uncertainty that the samples represent basal material, these elements are considered to be unreliable for the detailed detection of vein type mineralisation in such an environment. Levels of Ba in till increase with depth and are hence directly related to the horizon sampled. This is illustrated on Line A (Figure 12a) where the two major Ba peaks (Hole Nos. 3 and 6) coincide with the deepest samples.

Overall levels of Pb in deep tills ($\bar{x}$ = 760 ppm) are lower than those recorded for sub-surface soils ($\bar{x}$ = 980 ppm) but it appears to be the most reliable element in locating the position of the Rake. A distinct Pb anomaly is associated with the Long Rake on Lines B and C with a corresponding increase in Zn on both lines and an increase in Ba on Line C. Zn in general shows little contrast in deep tills but tends to have a similar dispersion pattern to Pb.

On Lines D and E, Zn shows better contrast when compared to Lines A, B and C, and an increase in concentration towards the north. It is considered that this is due to hydromorphic dispersion downslope due to leaching of Zn from the vein. Also, the sphalerite content of the vein is variable along strike and it is possible that it increases in the vicinity of Lines D and E. Zn is

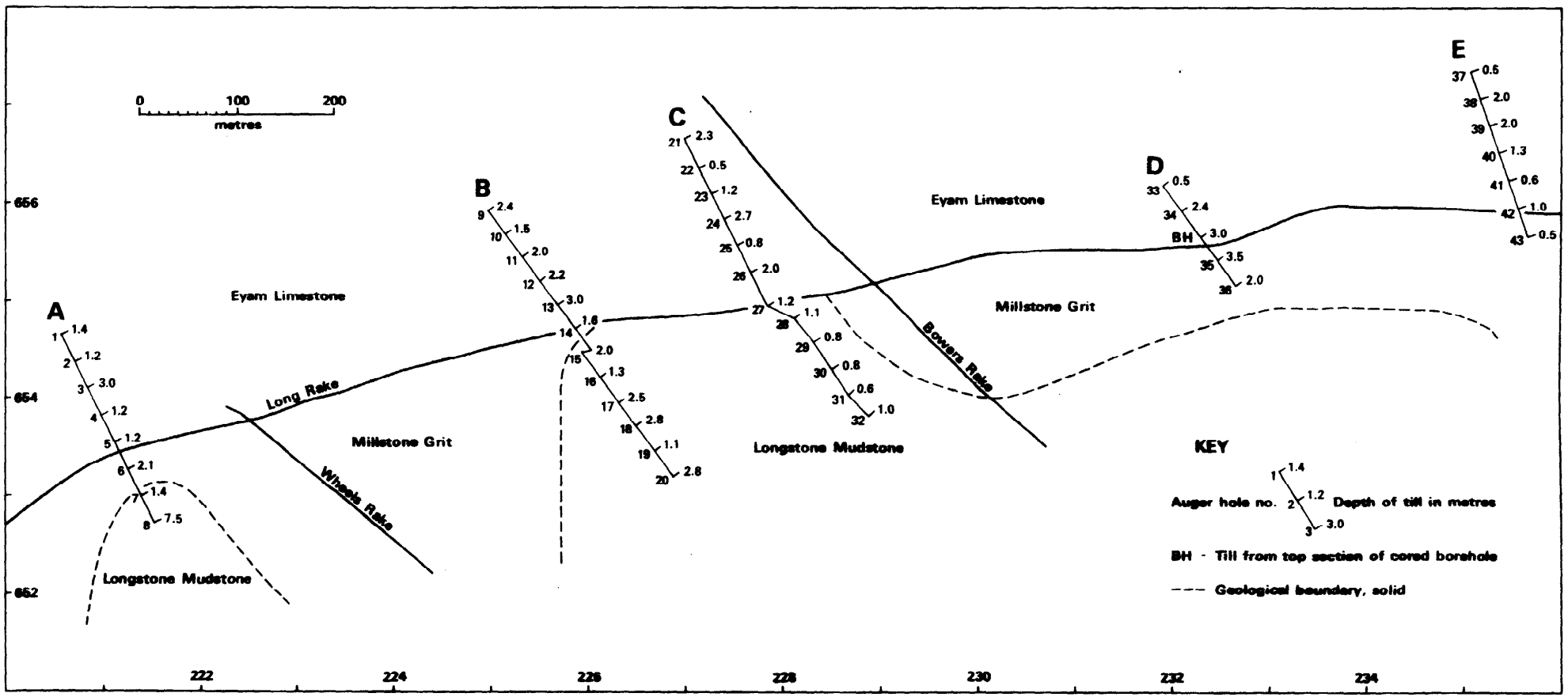

Figure 11 Location of till sample lines

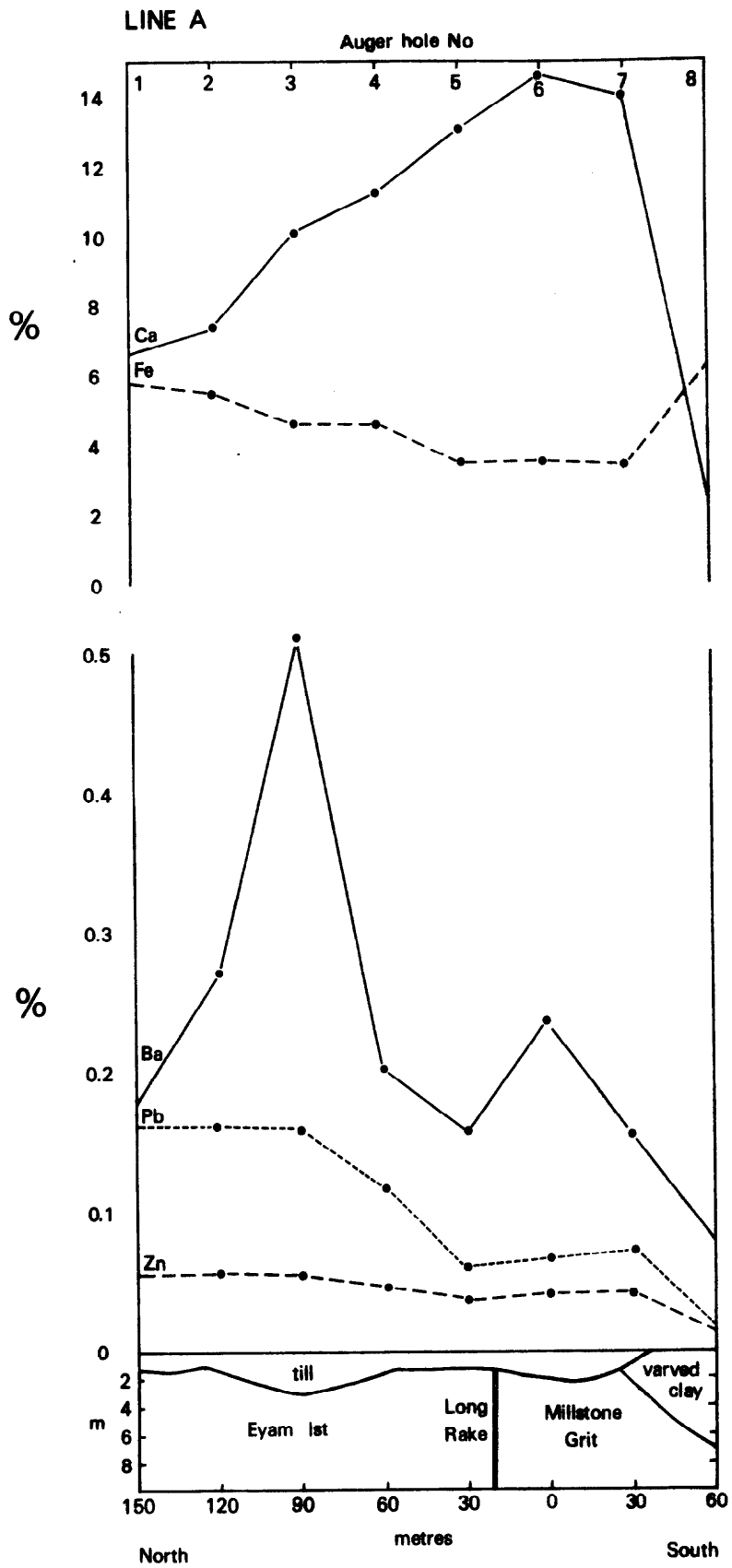

Figure 12a Dispersion of elements in deep tills Line A (see Figure 11 for location)

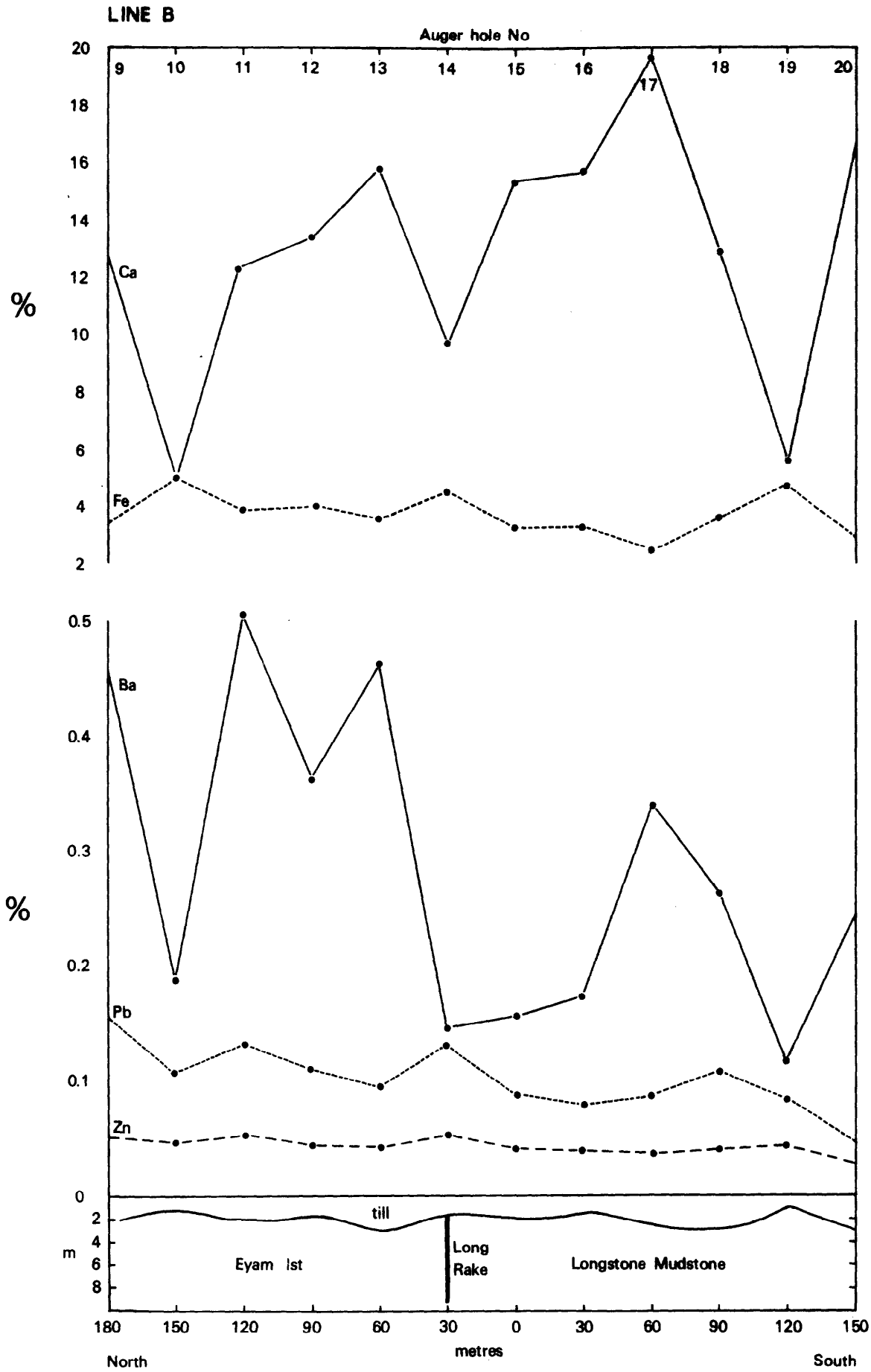

Figure 12b Dispersion of elements in deep tills Line B
(see Figure 11 for location)

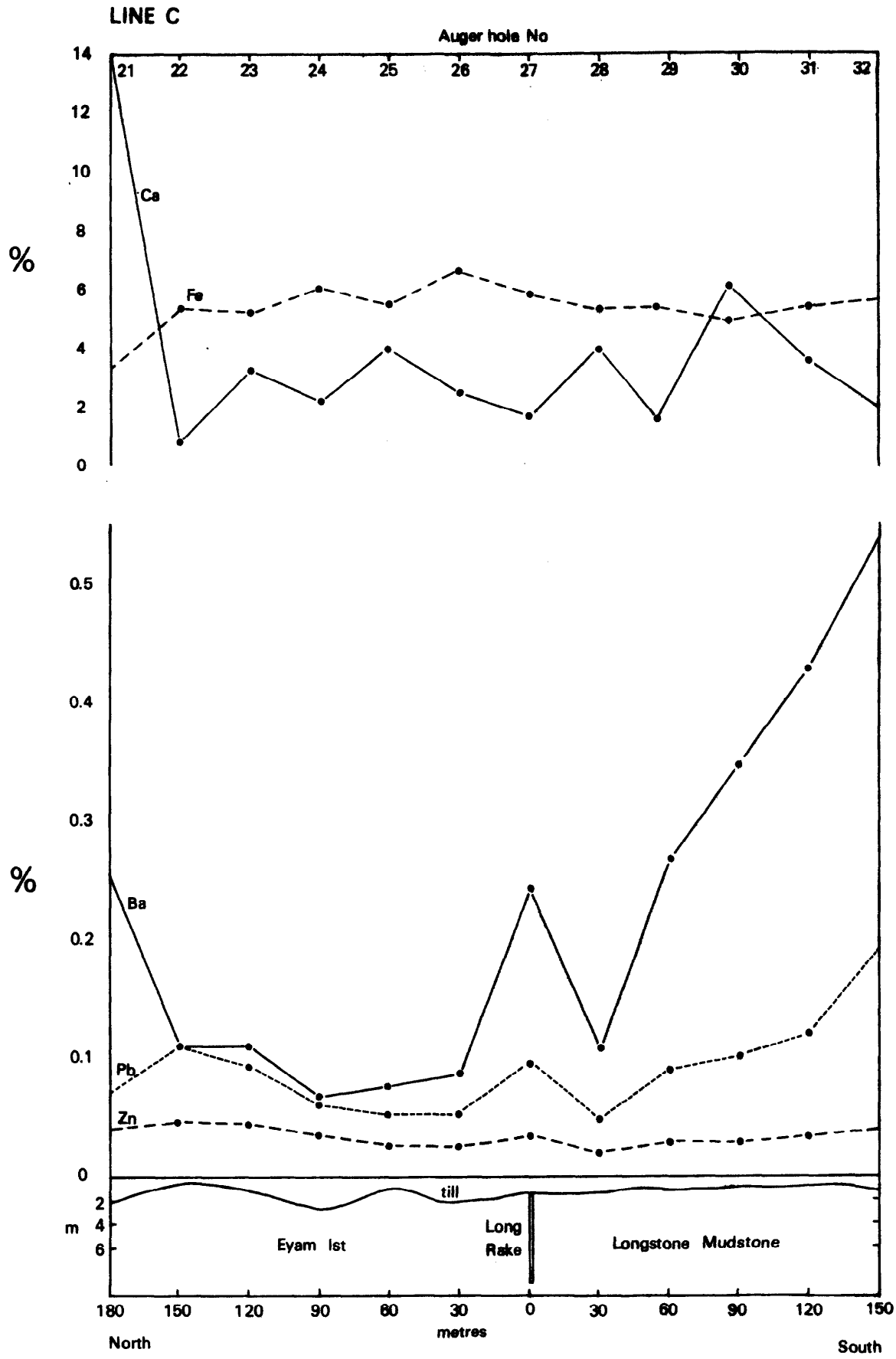

Figure 12c Dispersion of elements in deep tills Line C
(see Figure 11 for location)

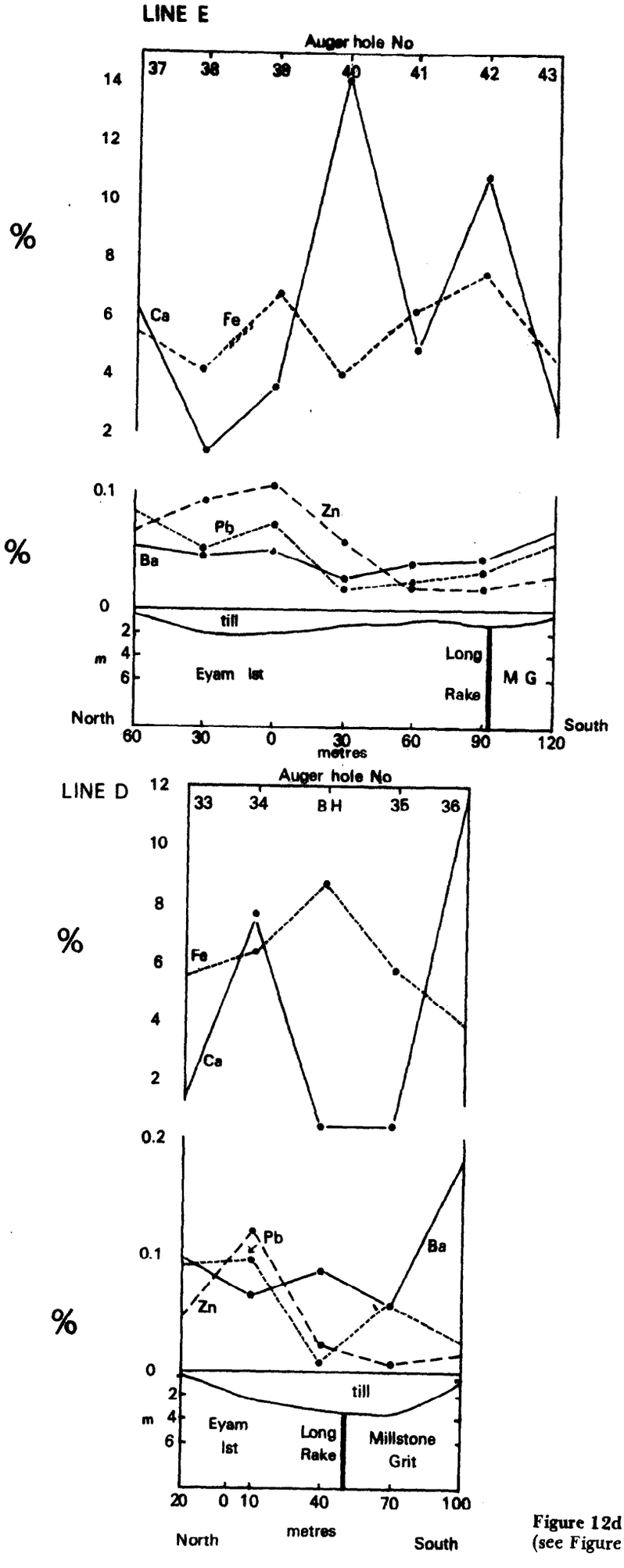

Figure 12d Dispersion of elements in deep tills Lines D and E (see Figure 11 for location)

Table 5 Summary statistics comparing deep tills with sub-surface soils

Element	Sub-surface soils n = 33		Deep tills n = 33	
	$\bar{x}$ $\log_{10}$	σ	$\bar{x}$ $\log_{10}$	σ
Ca	2.55%	0.44	7.24%	0.39
Ti	5620	0.08	4240	0.11
Mn	860	0.16	810	0.18
Fe	5.3%	0.90	4.5%	0.12
Ni	90	0.12	99	0.10
Cu	56	0.07	62	0.15
Zn	380	0.18	400	0.24
As	15	0.15	12	0.32
Pb	80	0.10	65	0.16
Sr	118	0.14	192	0.16
Y	42	0.10	40	0.15
Zr	260	0.09	175	0.12
Nb	13	0.07	11	0.08
Mo	3	0.67	6	0.27
Ag	0.5	1.60	0.2	1.66
Sn	0.5	1.66	0.2	1.66
Sb	5	1.64	5	1.59
Ba	1220	0.28	1490	0.35
Ce	45	0.10	36	0.18
Pb	730	0.23	690	0.34
Th	9	0.08	7	0.13
U	4	0.68	6	0.21

Values in ppm except where otherwise indicated

less highly concentrated in deep tills ($\bar{x}$ = 400 ppm) overall when compared to sub-surface soils ($\bar{x}$ = 460 ppm).

A marked depletion of Ca, Ba, Pb and Zn to the south of Line A (Hole No. 8, Figure 12a) and an increase in Fe marks a change in the overburden to a thick deposit of varved clay.

ANOMALY PATTERNS IN TILL PROFILES

Table 5 gives summary statistics relating mean levels of elements in B–horizon sub-surface soils with deep and basal till samples collected from the same profile.

Each element determined for the 33 profiled holes was plotted in graphical form (not illustrated) to examine the change in concentration with depth. The number of samples collected down the till profile varied between 2 and 10 and was dependent on till depth and texture/colour changes. Where no apparent change in till type was recognisable samples were taken at 0.5 m intervals down the profile.

Many elements showed no distinct patterns, but an overall increase in the levels of Cu, Sb, Mo, Ni and Sr was evident with depth. A very marked decrease in the level of Zr accompanied an increase in depth, with a less pronounced decrease of Ti, Rb and Th. Ba, Pb, Zn, As, Fe, Mn, Nb, Ce and Y showed variable patterns throughout the till profiles.

Comparisons were made between the levels of Ca, Fe, Ba, Pb and Zn in deep tills and B–horizon sub-surface soils along Lines A and B (Figure 13). Data were derived from profiled holes sampled from surface down to the bedrock/till interface where possible.

Pb and Zn show similar levels and similar dispersion patterns in the deep tills and sub-surface soils. The dispersion of Ba is more variable and exhibits higher levels in the deep tills, but overall shows a similar pattern to the soils. Similarly Ca is more highly concentrated in deep tills but again the data are somewhat variable, producing no distinct pattern. The dispersion pattern of Ca is similar for both sample types along Line B but a correlation is not so apparent on Line A (Figure 13). Levels of Fe are slightly higher in the sub-surface soils but the dispersion patterns are broadly similar.

The anomaly patterns in both sample types indicate that there is no advantage in collecting deep till samples, as geochemical contrast in the five elements examined is not improved.

CONCLUSIONS

1 Gravity measurements show that a minor Bouguer anomaly low is associated with the Long Rake structure and that gravimetric measurements could be used to locate a vein of approximately known position. However, a Bouguer anomaly low does not imply the presence of mineralisation and this factor, coupled with the high operating costs and the comparatively low density of the fluorite, renders gravity surveys unsuitable for routine exploration.

2 The magnetic results indicated that, given adequate control, useful structural information might be obtained concerning the depth and disposition of the controlling toadstone. Refined quantitative interpretations will need to consider the possible influence of remanent magnetisation.

3 EM and DC resistivity profiling techniques failed to produce anomalies that could be attributed to the fluorspar vein or the fault zone. Similarly the absence of any IP response downgrades the possibility of significant sulphides being present. Considerable variations in the response of fluorspar veins have been noted by other workers (Coney and Myers, 1977) and the absence of anomalies does not imply that electrical methods will be unsuitable in other areas. Limited success was obtained with the VLF/Radiohm methods in mapping the fluorspar vein by its association with the subdrift shale/limestone contact.

4 Reliable information was obtained on the drift lithologies and depth to bedrock using VES, but future investigations should consider the use

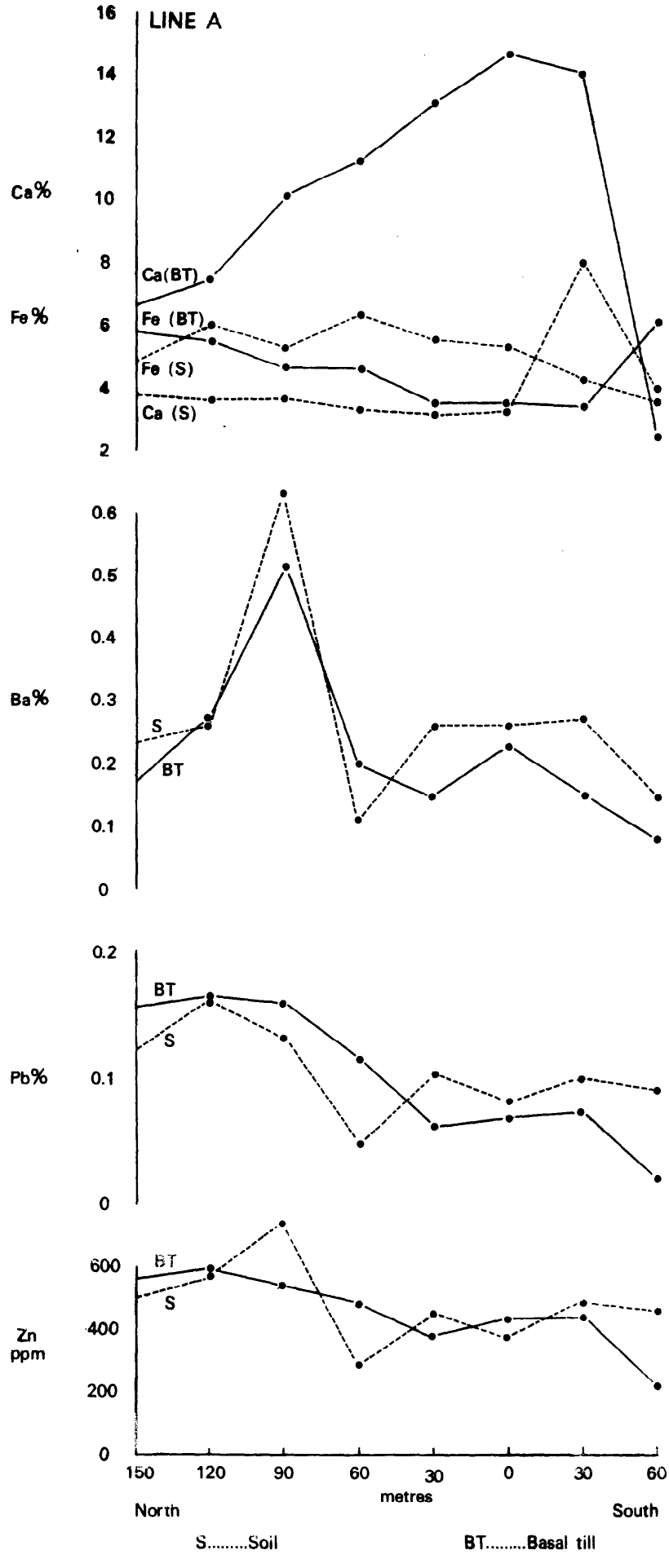

Figure 13a Comparison of element distribution in deep tills and sub-surface soils Line A (see Figure 11 for location)

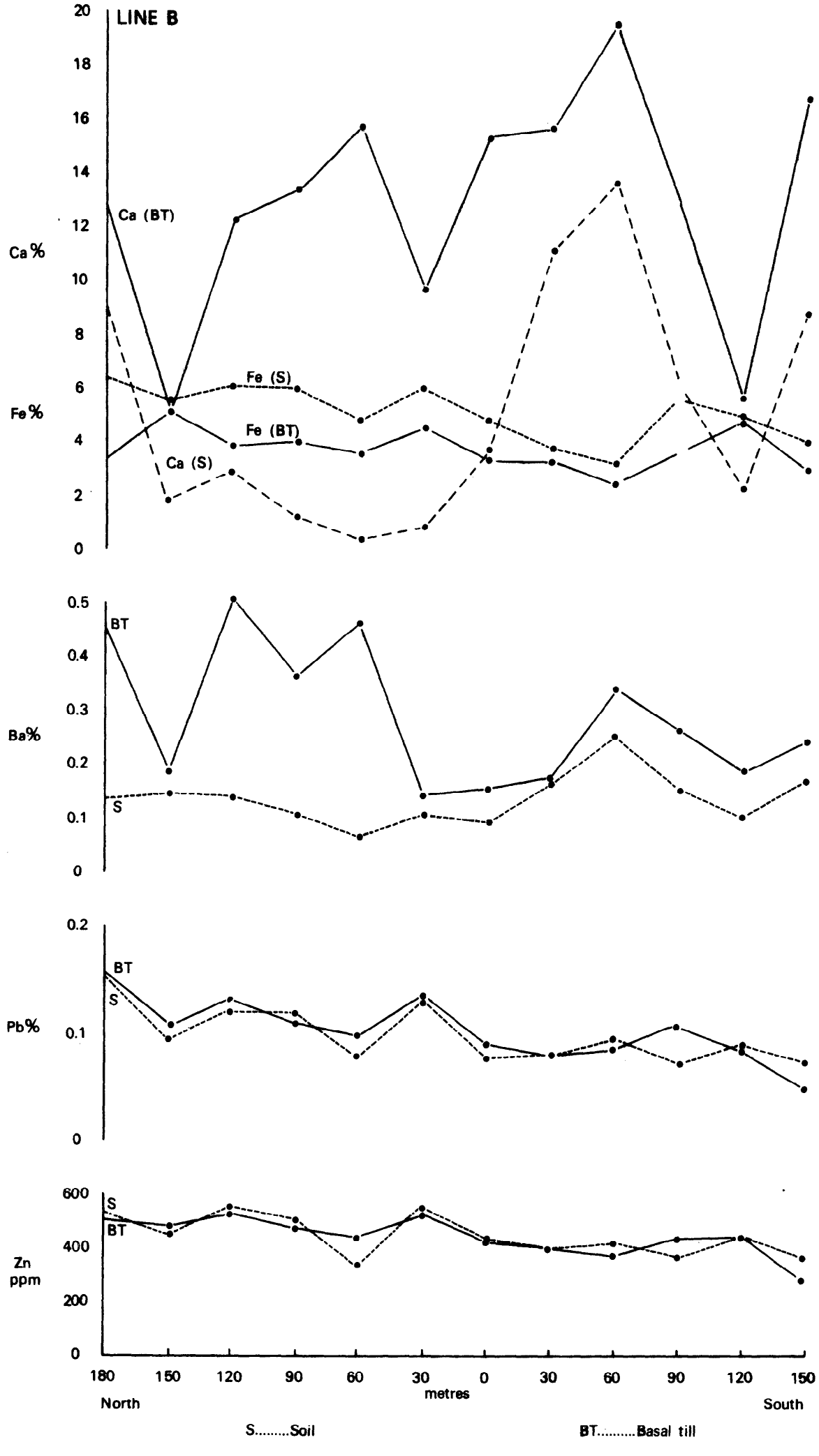

Figure 13b Comparison of element distribution in deep tills and sub-surface soils Line B (see Figure 11 for location)

of EM sounding methods.

5 In areas of shallow overburden the sub-outcrop of the vein can be mapped geochemically, based on levels of Pb, Ba, Sr, Zn, Ca, Rb and Th in soils. However, in areas of deep till only Pb, Ba and Sr are anomalous in sub-surface soils but the dispersion pattern is broad and fails to indicate a precise location for the mineral vein.

6 The mobile elements Zn and F are widely dispersed in soils in the vicinity of the mineralisation. The use of F as an indicator of F, Ba, Pb and Zn mineralisation in soils is particularly useful during the reconnaissance stage of a survey, due to the availability of rapid partial and total fluoride extraction methods, followed by analysis using a specific ion electrode.

7 The collection and analysis of deep till samples fails to improve geochemical contrast in areas of deep overburden.

8 Sub-outcropping black shales are identifiable by the increase over background levels of Ni, Cu, As, Mo, U and Ce/Y ratios in soils. High levels of U in soil are associated with the uraniferous *Cravenoceras leion* marine band.

ACKNOWLEDGEMENTS

The Institute is indebted to Dresser Minerals International UK, based at Hopton, Derbyshire, for the use of geological information and access to drill core for sampling and geophysical measurements. The authors particularly wish to thank N. J. Butcher who gave much advice on the detailed geology of the area. The Institute is also grateful to Haddon Estates for their co-operation in permitting access to the ground to collect samples.

The authors wish to thank D. Patrick, T. K. Ball and G. Easterbrook for assistance in the field, B. R. H. Skilton for mineralogical examination of drill cores, T. K. Smith for the analysis of soil and till samples and members of the Keyworth and London drawing offices who prepared the diagrams. J. I. Chisholm provided critical advice on the geology and mineralisation section.

REFERENCES

Al Atia, M. J. and Barnes, J. W. 1976. Rubidium: a primary dispersion pathfinder at Ogofau gold mine, southern Wales. In **Elliott, I. L. and Fletcher, W. K.** (editors) *Geochemical Exploration 1974.* (Amsterdam: Elsevier), pp. 341–352 (*Ass. Explor. Geochem. Spec. Publ. No. 2*).

Al-Kufaishi, F. A. M. 1969. *A mineralogical and geochemical study of part of Long Rake vein in the Derbyshire orefield.* MSc Thesis, University of Sheffield, Sheffield.

Bayrock, L. A. and Pawluk, S. 1967. Trace elements in tills of Alberta. *Canada J. Earth. Sci.*, Vol. 4, pp. 597.

Brown, M. J. and Ball, T. K. 1979. Gamma-ray spectrometric investigations over four selected non-radioactive mineral deposits. *Inst. Geol. Sci., MMAGU R. & D. Rep. No. 2* (unpublished).

Coney, D. P. and Myers, J. O. 1977. Some comparative field results for resistivity, very-low-frequency electromagnetic and horizontal-loop electromagnetic methods over fluorspar veins. *Trans. Instn. Min. Metall. (Sect. B: Appl. Earth Sci.)*, Vol. 86, pp. 1–3.

Dunham, K. C. 1952. Fluorspar. *4th edn. Spec. Miner. Resour. G.B. 4*, 143 p.

Farrell, B. L. 1974. Fluorine, a direct indicator of fluorite mineralisation in local and regional soil geochemical surveys. *J. Geochem. Expl.*, Vol. 3, pp. 227–244.

Ficklin, W. J. 1970. A rapid method for the determination of fluoride in rocks and soils, using an ion-selective electrode. *US Geol. Surv. Prof. Paper*, No. 700C: C186–188.

Firman, R. J. and Bagshaw, C. A. 1974. A re-appraisal of the controls of non-metallic gangue mineral distribution in Derbyshire. *Mercian Geol.*, Vol. 5, pp. 145–161.

Ford, T. D. 1967. The stratiform ore deposits of Derbyshire. In **James, C. H.** (editor) *Sedimentary ores* (Proc. 15th inter-university geological congress, Leicester) (Leicester: Dept. of Geol. University of Leicester 1969) pp. 73–93.

— **and Ineson, P. R.** 1971. The fluorspar mining potential of the Derbyshire orefield. *Trans. Instn. Min. Metall. (Sect. B: Appl. Earth Sci.)*, Vol. 80, pp. B186–210.

Fraser, D. C. 1969. Contouring of VLF-EM data. *Geophysics*, Vol. 34, No. 6, pp. 958–967.

Ineson, P. R. and Mitchell, J. G. 1972. Isotopic age determinations on clay minerals from lavas and tuffs of the Derbyshire ore field. *Geol. Mag.*, Vol. 109, pp. 501–512.

Kumar, R. 1973. Resistivity type curves over outcropping vertical dyke II *Geophysical Prospecting*, Vol. 21, No. 4, pp. 615–625.

Lepeltier, C. 1969. A simplified statistical treatment of geochemical data by graphical representation. *Econ. Geol.*, Vol. 64, pp. 538–550.

Mason, J. E. 1973. Geology of the Derbyshire fluorspar deposits, United Kingdom. In **Hutcheson, D. W.** (editor) *A symposium on the geology of fluorspar – proceedings 9th forum on geology of industrial minerals Spec., Publs. Ky. Geol. Surv.*, No. 22, 107 p.

Masson Smith, D., Howell, P. M., Abernethy-Clark, A. B. D. E. and Proctor, D. W. P. 1974. The national gravity reference net 1973. *Professional Paper New Series No. 26*, Ordnance Survey of GB.

Moorbath, S. 1962. Lead isotope abundance studies on mineral occurrences in the British Isles and their geological significance. *Phil. Trans. R. Soc., London*, Vol. 254A, pp. 295–360.

Robinson, B. W. and Ineson, P. R. 1979. Sulphur, oxygen and carbon isotope investigations of lead-zinc-barite-fluorite-calcite mineralisation, Derbyshire, England. *Trans. Instn. Min. Metall. (Sect. B: Appl. Earth Sci.)*, Vol. 88, pp. B107–117.

Rogers, P. J. 1977. Fluid inclusion studies in fluorite from the Derbyshire orefield. *Trans. Instn. Min. Metall. (Sect. B: Appl. Earth Sci.)*, Vol. 86, pp. B128–132.

Sawkins, F. J. 1968. The significance of Na/K and Cl/SO_4 ratios in fluid inclusion and subsurface waters, with respect to the genesis of Mississippi Valley type ore deposits. *Econ. Geol.*, Vol. 63, pp. 935–942.

Schnellmann, G. A. and Wilson, J. D. 1947. Lead-zinc mineralisation in north Derbyshire. *Trans. Instn. Min. Metall.*, Vol. 56, pp. 549–585.

Smith, E. G., Rhys, G. H. and Eden, R. A. 1967. Geology

of the country around Chesterfield, Matlock and Mansfield: Explanation of one-inch sheet 112 (new series). *Mem. Geol. Surv. GB.*, 430 pp.

Smith, R. T. and Gallagher, M. J. 1975. Geochemical dispersion through peat and till from metalliferous mineralisation in Sutherland. In **Jones, M. J.** (editor) *Prospecting in areas of glaciated terrain, Instn. Min Metall.*, pp. 134–147.

Steed, G. M. and others. 1976. Geochemical and biogeochemical prospecting in the area of the Ogofau gold mines, Dyfed, Wales. *Trans. Instn. Min. Metall. (Sect. B: Appl. Earth Sci.)*, Vol. 85, pp. B109–117.

Stevenson, I. P. and Gaunt, G. D. 1971. Geology of the country around Chapel-en-le-Frith: Explanation of one-inch geological sheet 99, (new series) *Mem. Geol. Surv. GB.*, 444 p.

Varvill, W. W. 1959. The future of lead-zinc and fluorspar mining in Derbyshire. In *The future of non-ferrous mining in Great Britain and Ireland.* (London: Instn. Min. Metall.), pp. 175–203.

Vinogradov, A. P. 1959. *The geochemistry of rare and dispersal chemical elements in soils* (2nd edition) New York Consultants Bur. Enterpr. 209 p.

APPENDIX 1

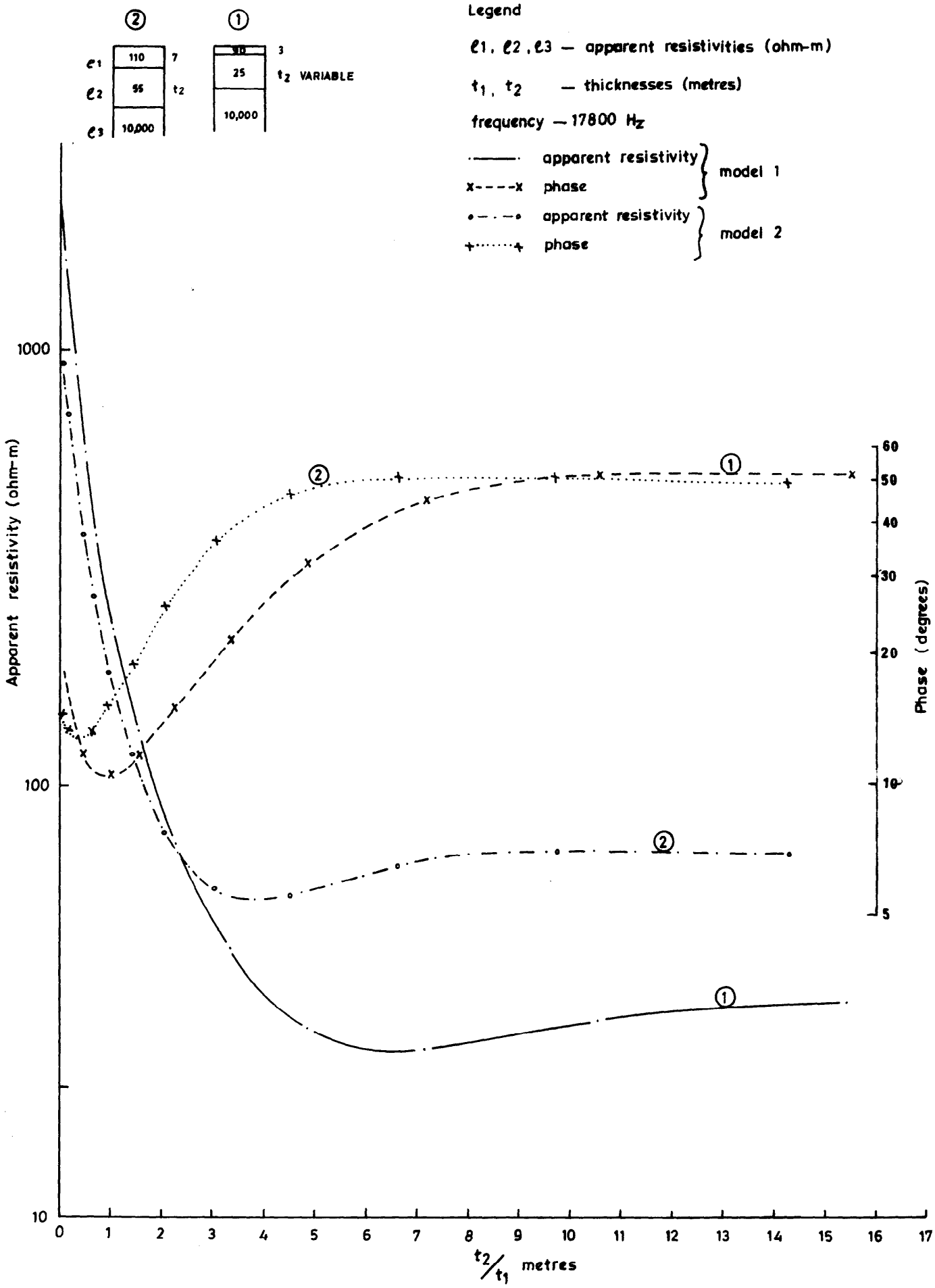

DEPENDENCE OF RADIOHM RESISTIVITY ON LAYER THICKNESS

Appendix 2 Geochemical maps of element distribution in soil

Calcium
Nickel
Copper
Zinc
Arsenic
Rubidium
Strontium
Yttrium
Molybdenum
Antimony
Barium
Cerium
Lead
Thorium
Uranium

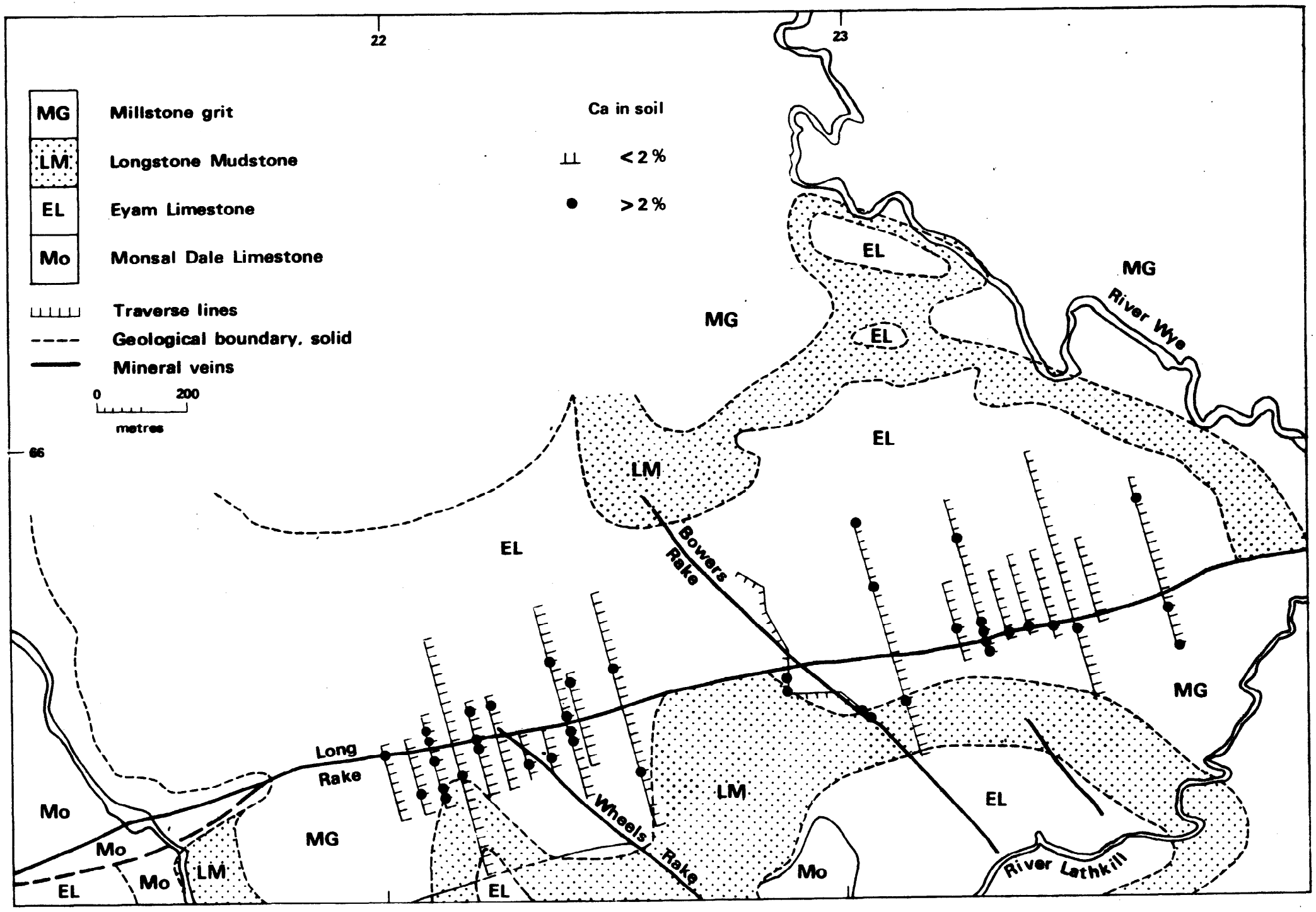
22
23
MG Millstone grit
LM Longstone Mudstone
EL Eyam Limestone
Mo Monsal Dale Limestone
Traverse lines
Geological boundary, solid
Mineral veins
0 200
metres
Ca in soil
<2%
>2%
66
MG
EL
LM
Mo
River Wye
Bowers Rake
Long Rake
Wheels Rake
River Lathkill

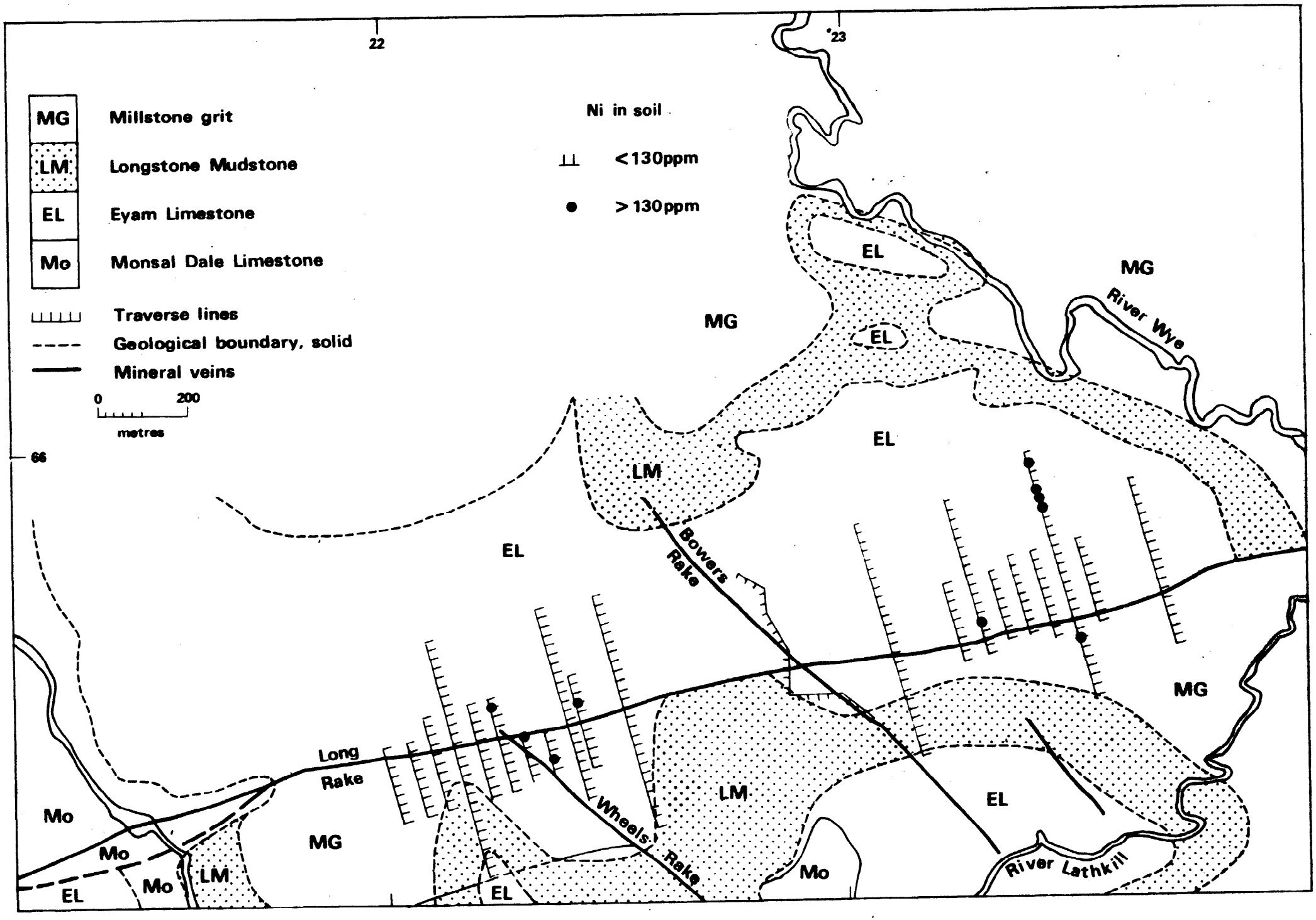
22
23
MG
Millstone grit
LM
Longstone Mudstone
EL
Eyam Limestone
Mo
Monsal Dale Limestone
Traverse lines
Geological boundary, solid
Mineral veins
0
200
metres
Ni in soil
<130ppm
>130ppm
66
32
River Wye
Bowers Rake
Long Rake
Wheels Rake
River Lathkill

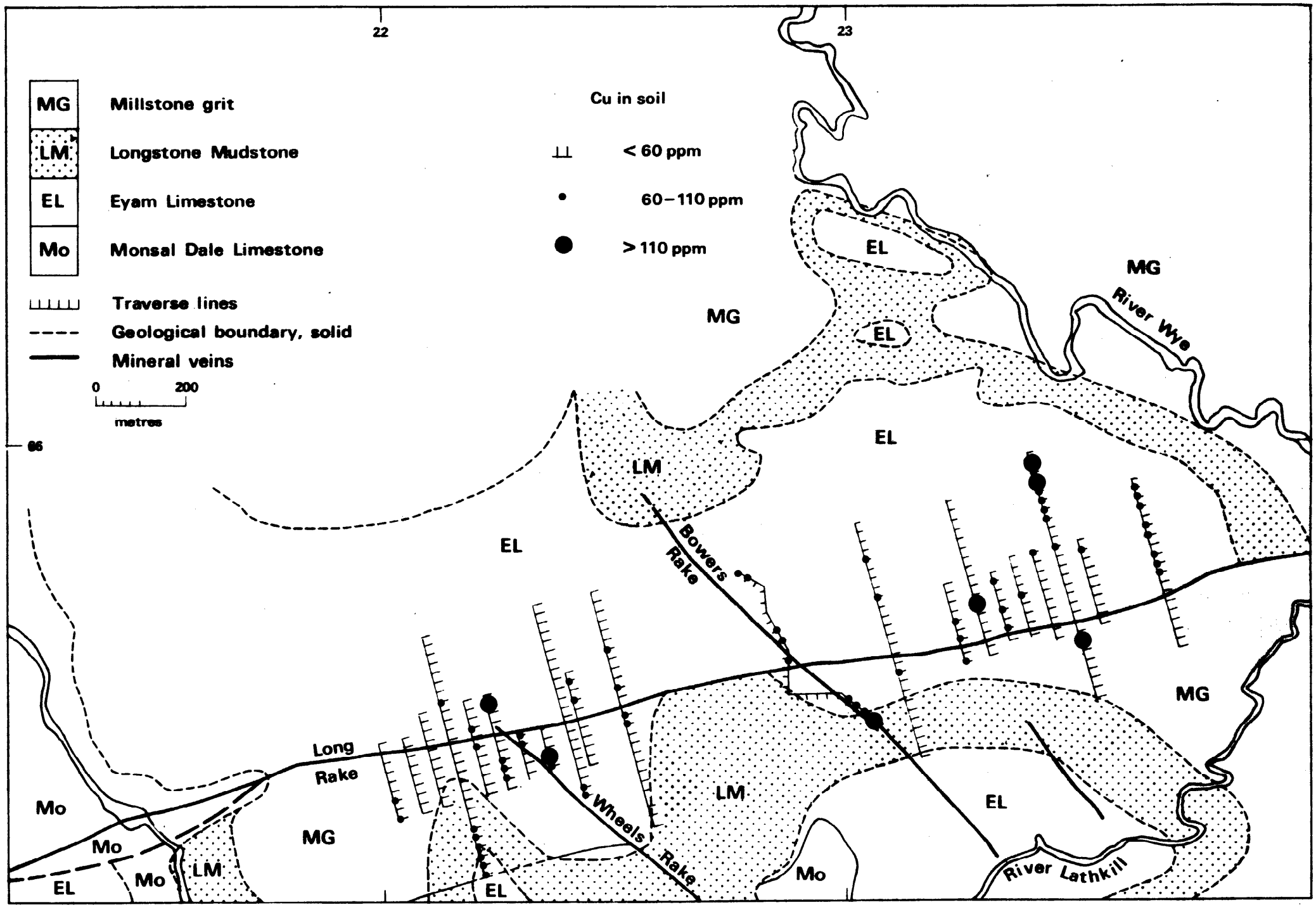
22
23
MG Millstone grit
LM Longstone Mudstone
EL Eyam Limestone
Mo Monsal Dale Limestone
Traverse lines
Geological boundary, solid
Mineral veins
0 200
metres
Cu in soil
< 60 ppm
60–110 ppm
> 110 ppm
06
River Wye
Bowers Rake
Long Rake
Wheels Rake
River Lathkill
MG
EL
LM
Mo

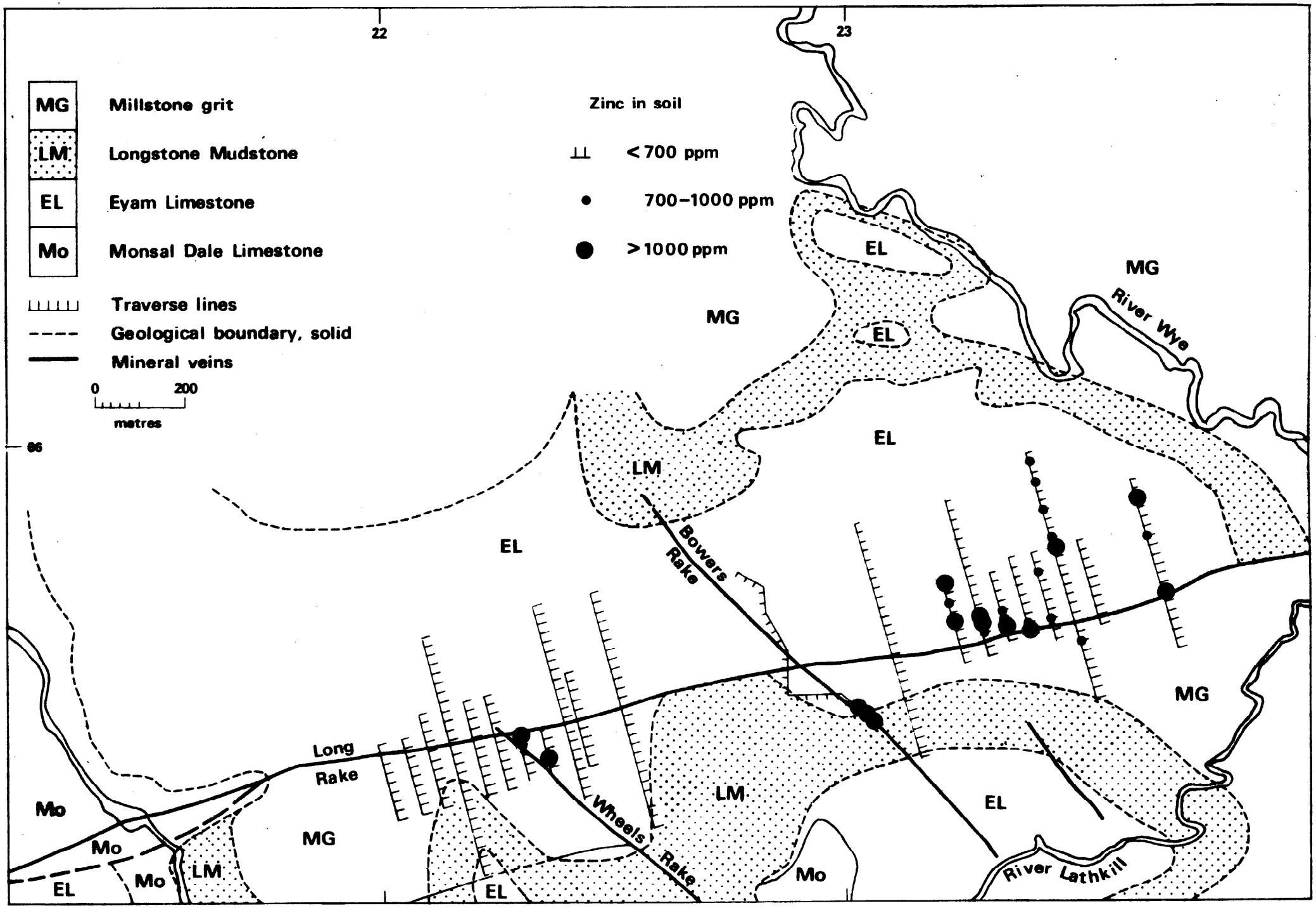
22
23
MG Millstone grit
LM Longstone Mudstone
EL Eyam Limestone
Mo Monsal Dale Limestone
Traverse lines
Geological boundary, solid
Mineral veins
0 200
metres
Zinc in soil
< 700 ppm
700–1000 ppm
> 1000 ppm
86
MG
EL
River Wye
LM
Bowers Rake
Long Rake
Wheels Rake
River Lathkill
Mo

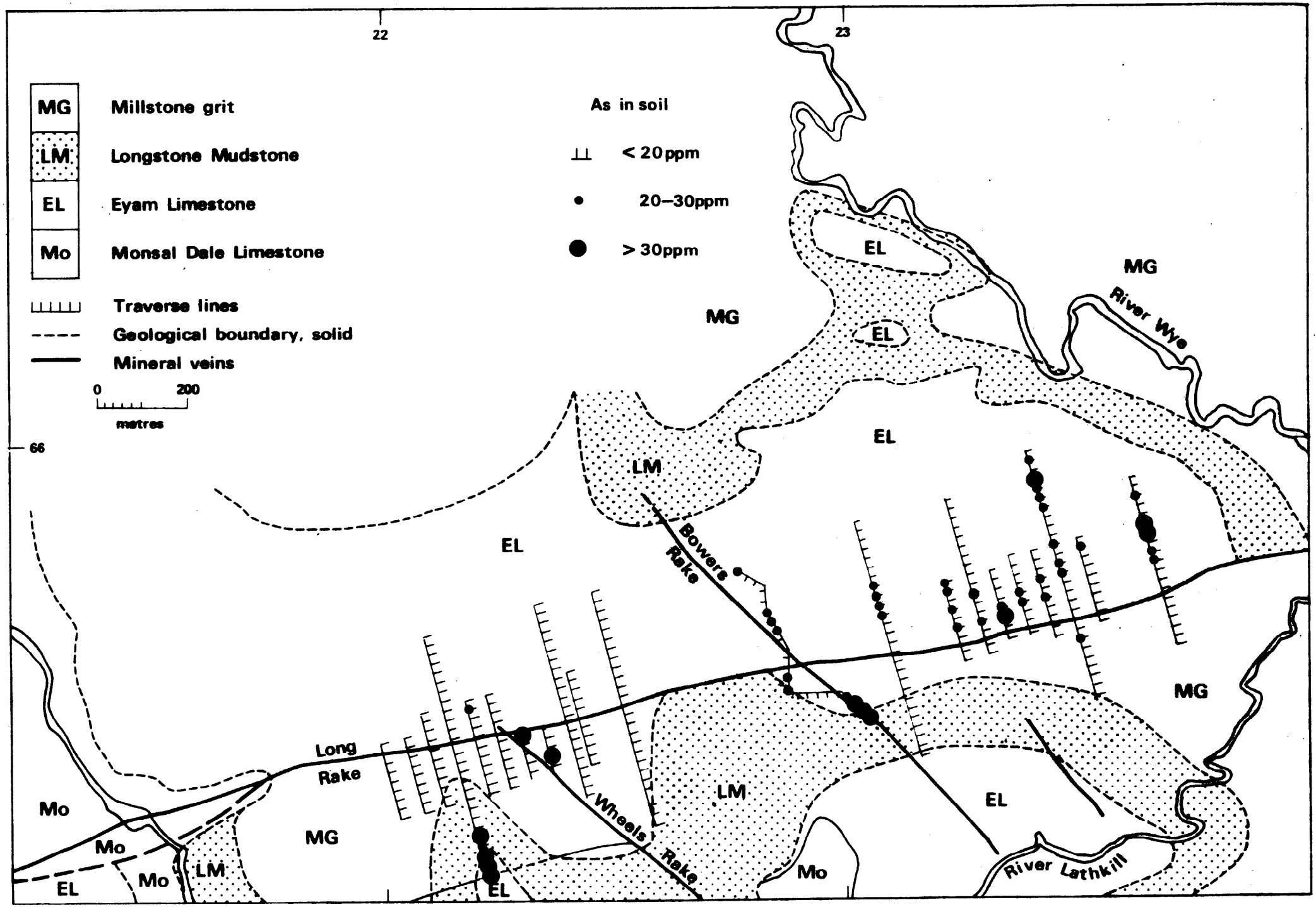
22
23
MG
Millstone grit
LM
Longstone Mudstone
EL
Eyam Limestone
Mo
Monsal Dale Limestone
Traverse lines
Geological boundary, solid
Mineral veins
0
200
metres
As in soil
< 20ppm
20–30ppm
> 30ppm
66
River Wye
Bowers Rake
Long Rake
Wheels Rake
River Lathkill

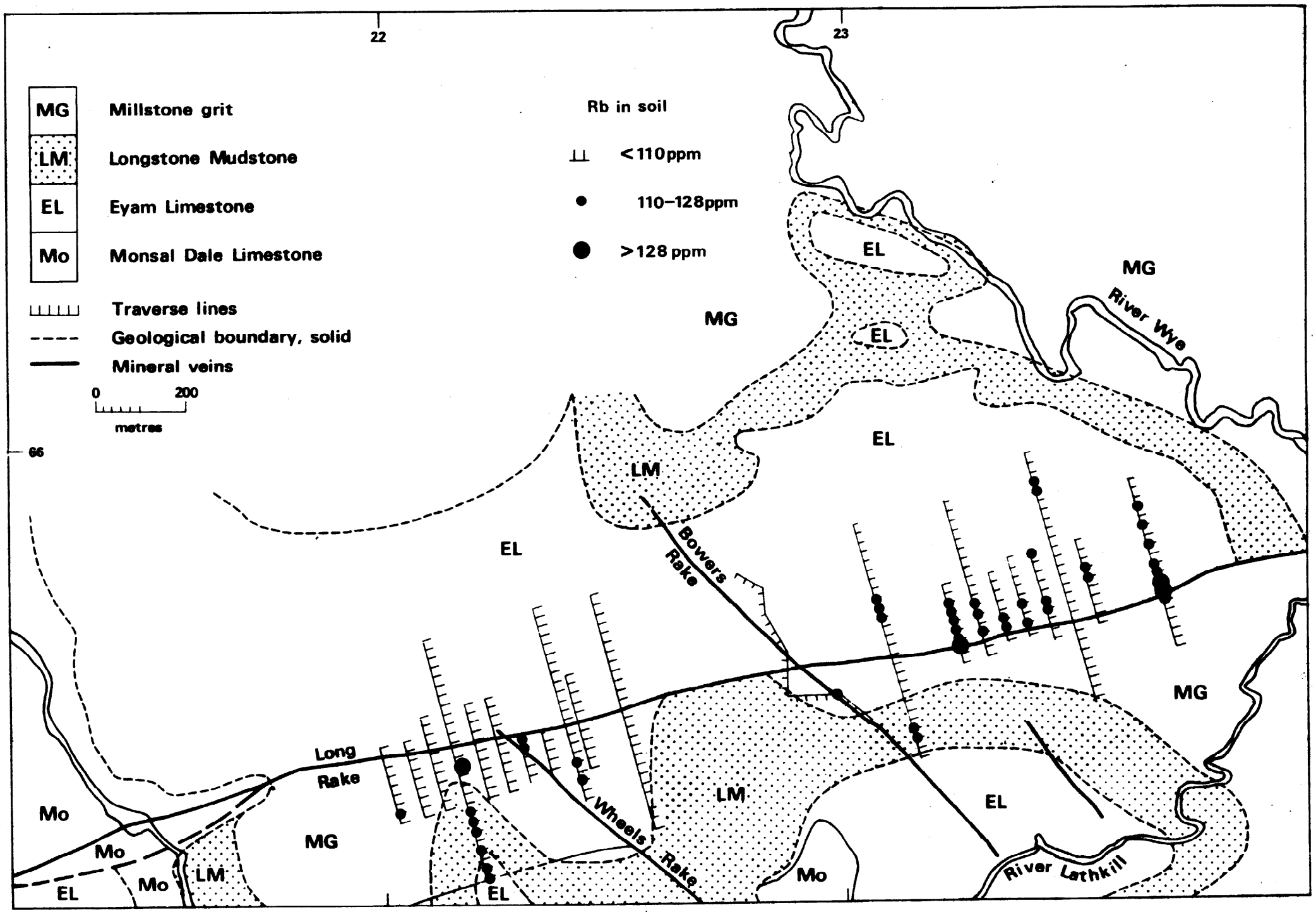
22
23
MG Millstone grit
LM Longstone Mudstone
EL Eyam Limestone
Mo Monsal Dale Limestone
Traverse lines
Geological boundary, solid
Mineral veins
0 200
metres
Rb in soil
<110ppm
110–128ppm
>128 ppm
66
MG
EL
LM
Mo
River Wye
Bowers Rake
Long Rake
Wheels Rake
River Lathkill

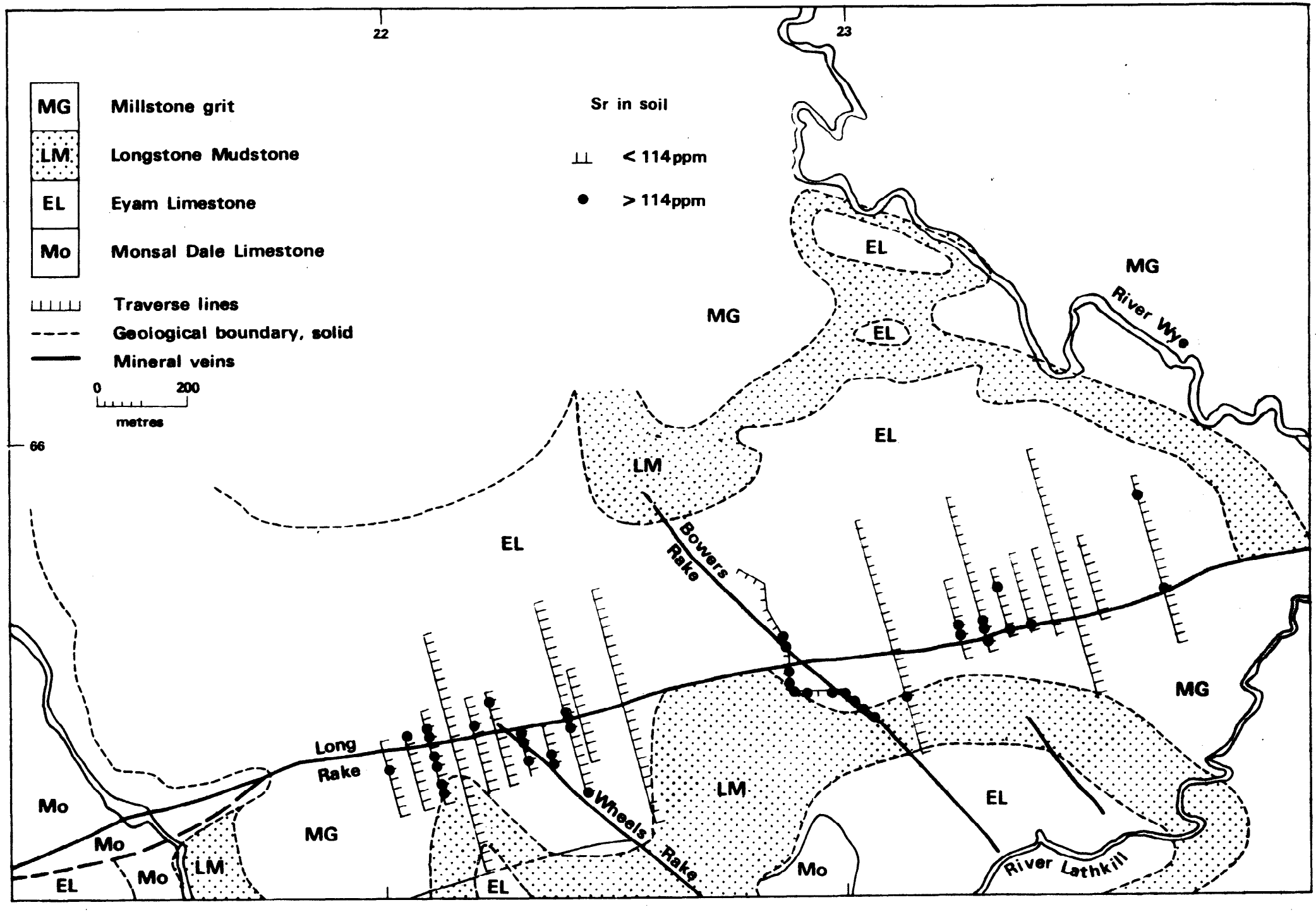
22
23
MG Millstone grit
LM Longstone Mudstone
EL Eyam Limestone
Mo Monsal Dale Limestone
Traverse lines
Geological boundary, solid
Mineral veins
0 200
metres
Sr in soil
< 114ppm
> 114ppm
66
37
MG
EL
LM
Mo
River Wye
River Lathkill
Bowers Rake
Long Rake
Wheels Rake

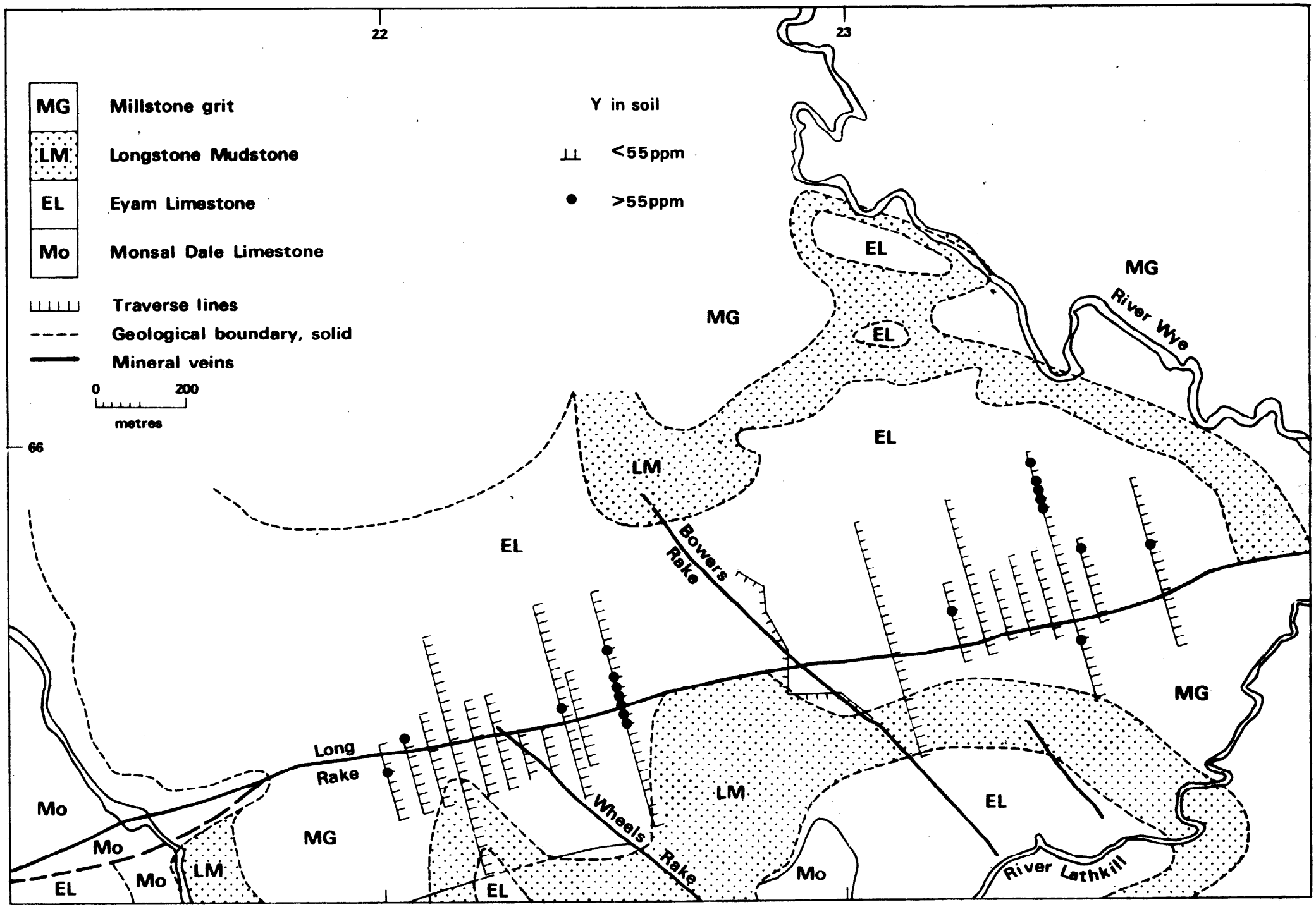
22
23
MG
Millstone grit
LM
Longstone Mudstone
EL
Eyam Limestone
Mo
Monsal Dale Limestone
Traverse lines
Geological boundary, solid
Mineral veins
0
200
metres
Y in soil
<55ppm
>55ppm
66
MG
EL
River Wye
LM
Bowers Rake
Long Rake
Wheels Rake
River Lathkill
Mo

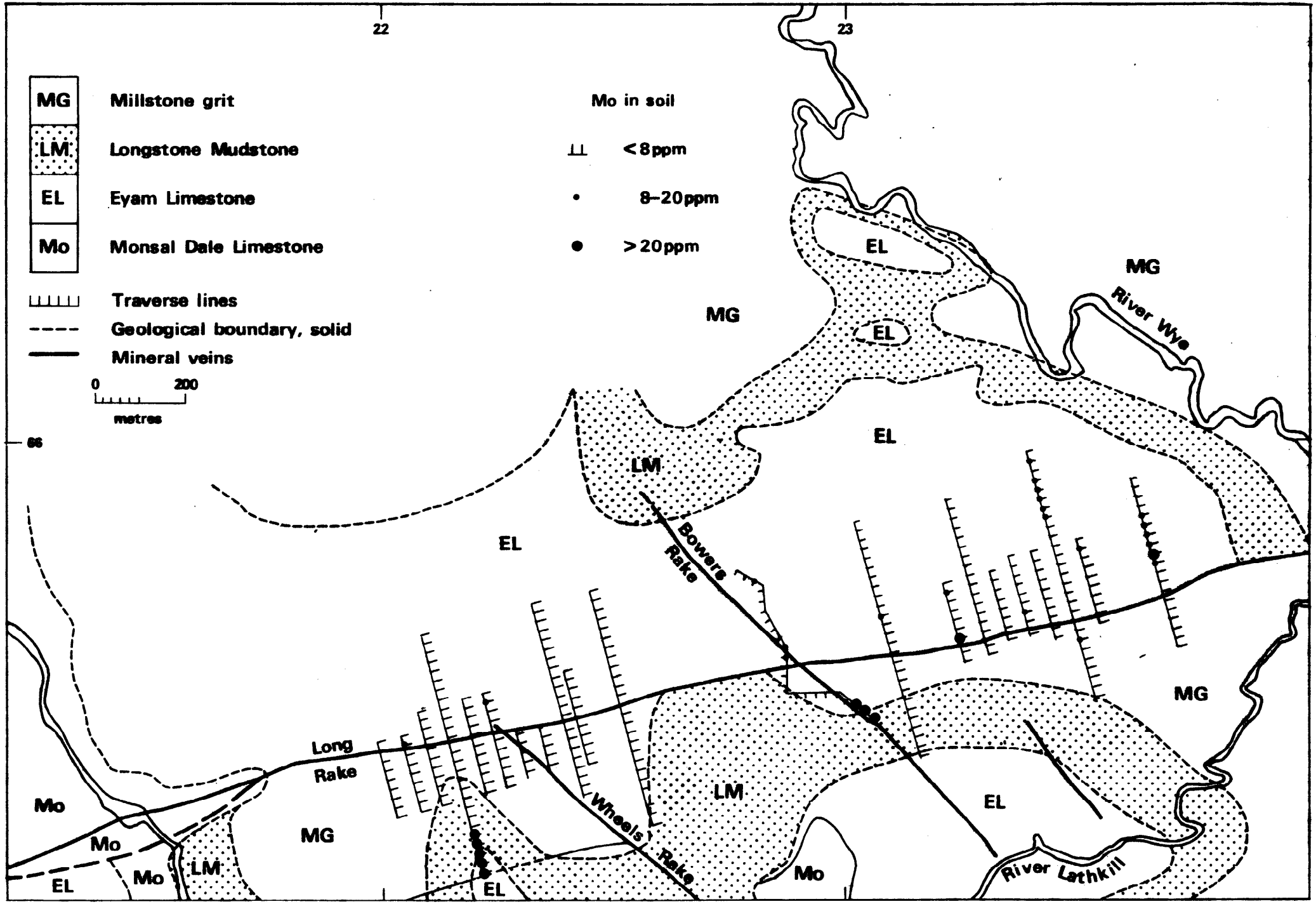
22
23
MG
Millstone grit
LM
Longstone Mudstone
EL
Eyam Limestone
Mo
Monsal Dale Limestone
Traverse lines
Geological boundary, solid
Mineral veins
0
200
metres
Mo in soil
<8ppm
8–20ppm
>20ppm
River Wye
Bowers Rake
Long Rake
Wheels Rake
River Lathkill
66

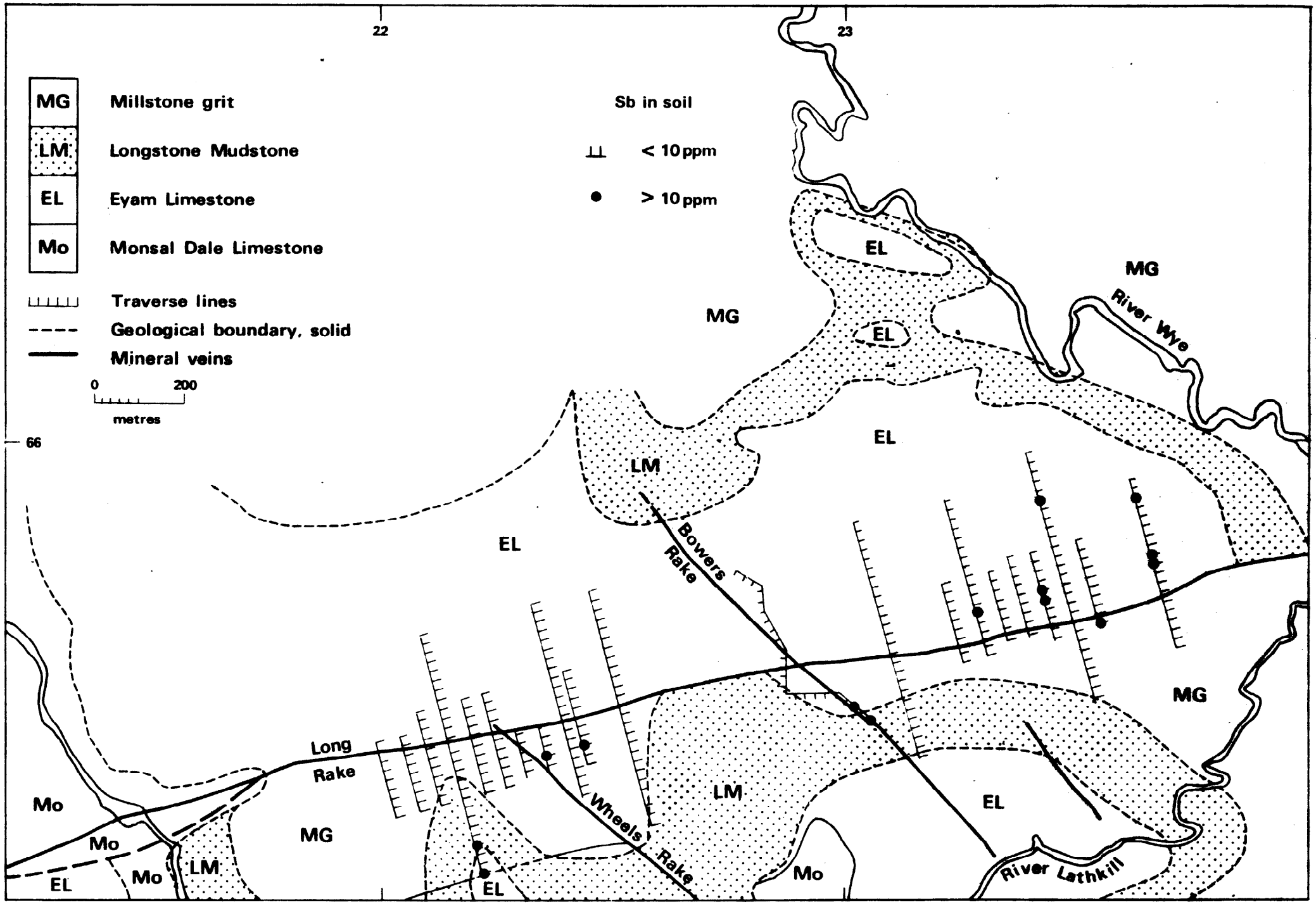
22
23
MG
Millstone grit
LM
Longstone Mudstone
EL
Eyam Limestone
Mo
Monsal Dale Limestone
Traverse lines
Geological boundary, solid
Mineral veins
0
200
metres
Sb in soil
< 10ppm
> 10ppm
66
River Wye
Bowers Rake
Long Rake
Wheels Rake
River Lathkill

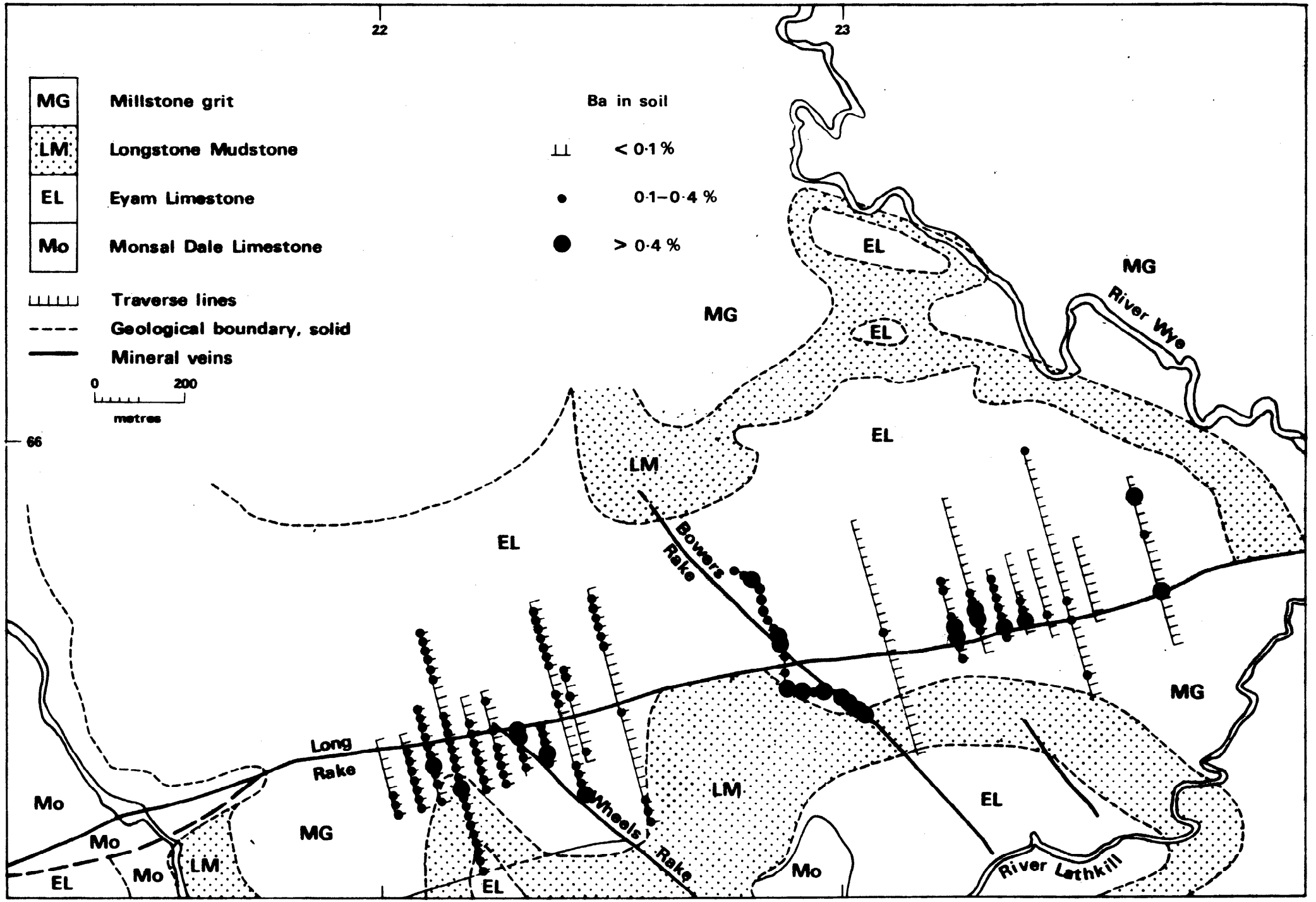
22
23
MG
Millstone grit
LM
Longstone Mudstone
EL
Eyam Limestone
Mo
Monsal Dale Limestone
Traverse lines
Geological boundary, solid
Mineral veins
0
200
metres
Ba in soil
< 0·1 %
0·1–0·4 %
> 0·4 %
66
River Wye
Bowers Rake
Long Rake
Wheels Rake
River Lathkill

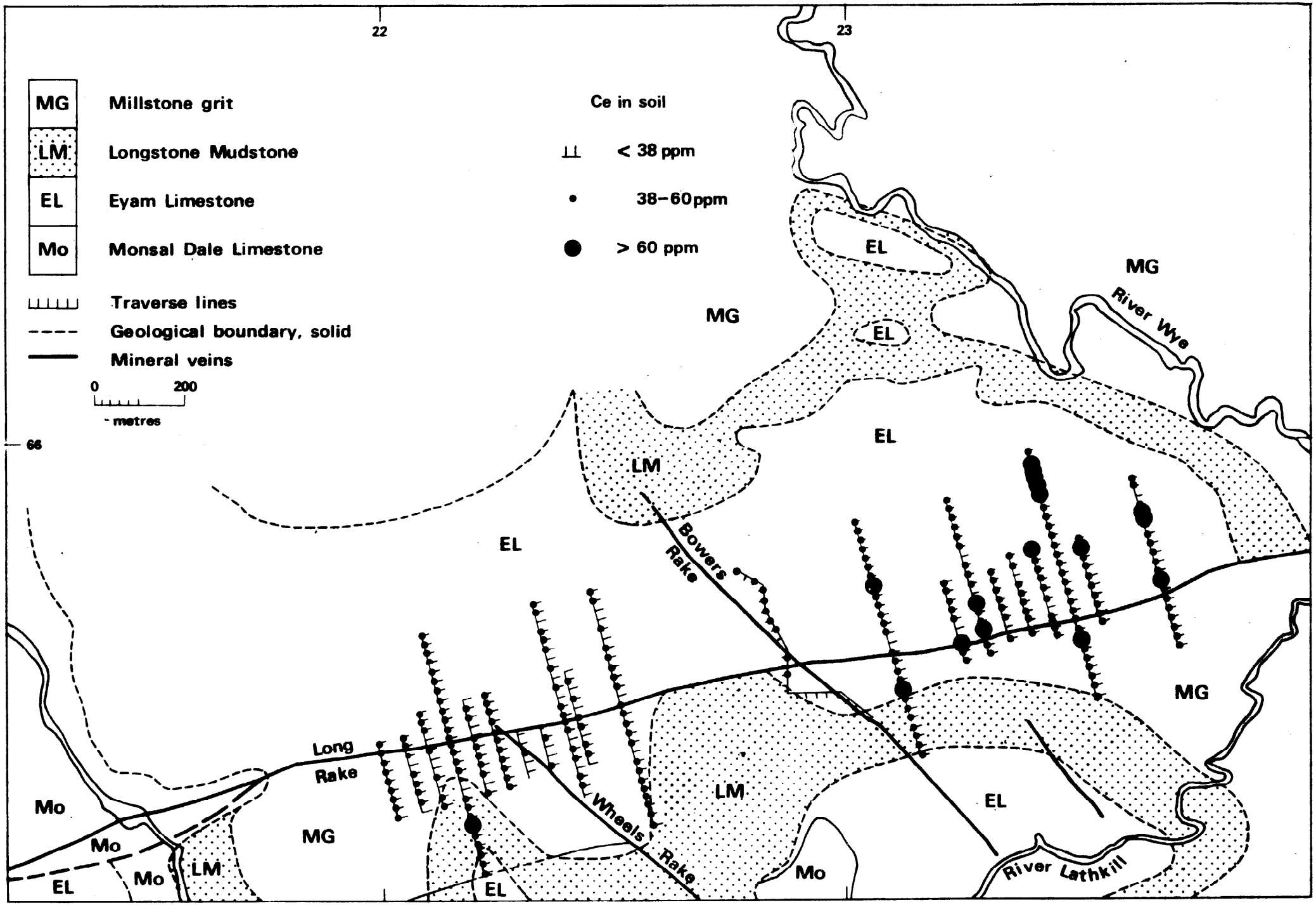
22
23
MG Millstone grit
LM Longstone Mudstone
EL Eyam Limestone
Mo Monsal Dale Limestone
Traverse lines
Geological boundary, solid
Mineral veins
0 200
metres
Ce in soil
< 38 ppm
38–60ppm
> 60 ppm
66
42
MG
EL
LM
Mo
River Wye
Bowers Rake
Long Rake
Wheels Rake
River Lathkill

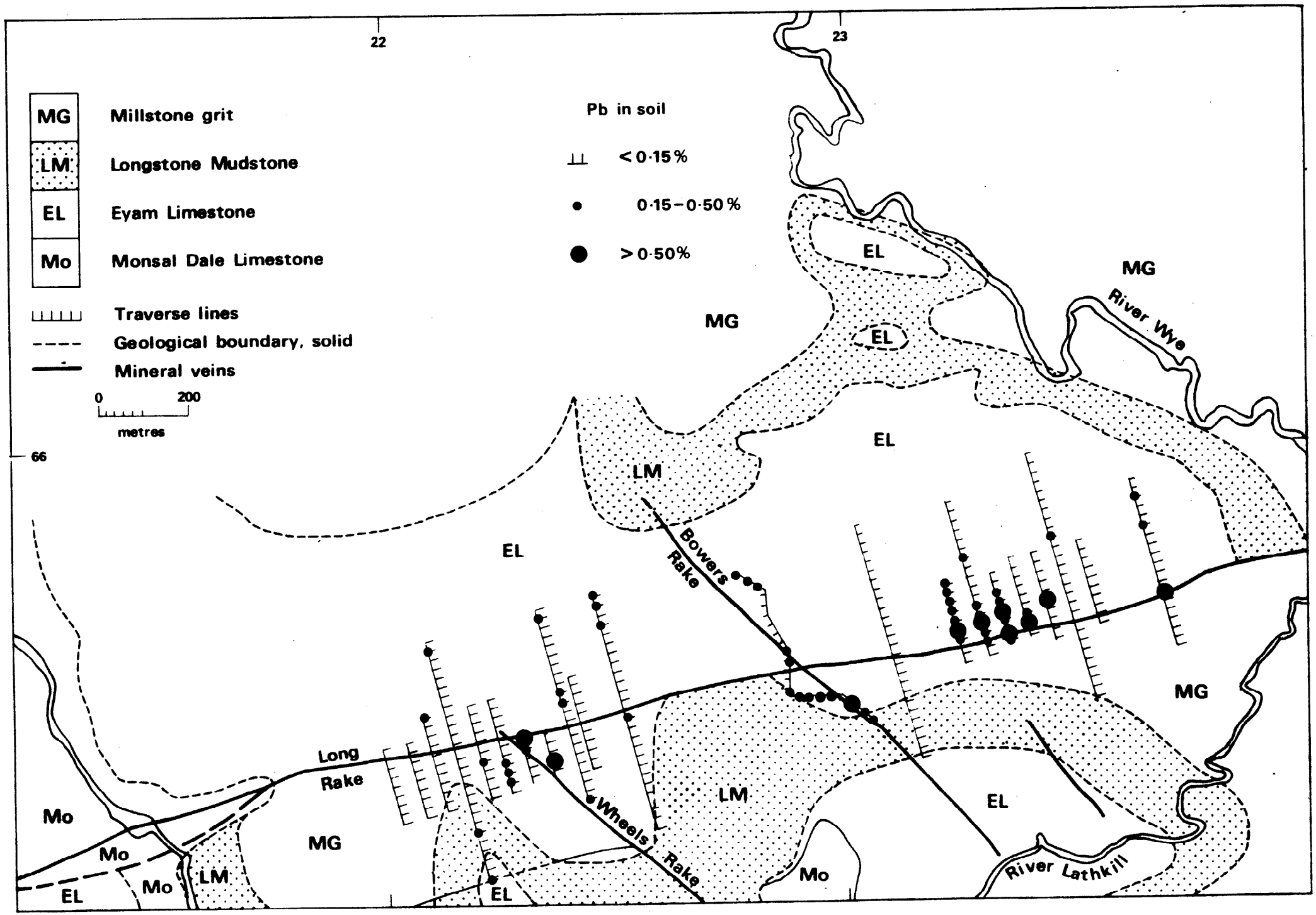
22
23
MG Millstone grit
LM Longstone Mudstone
EL Eyam Limestone
Mo Monsal Dale Limestone
Traverse lines
Geological boundary, solid
Mineral veins
0 200
metres
Pb in soil
< 0·15%
0·15–0·50%
> 0·50%
66
River Wye
Bowers Rake
Long Rake
Wheels Rake
River Lathkill
MG
EL
LM
Mo

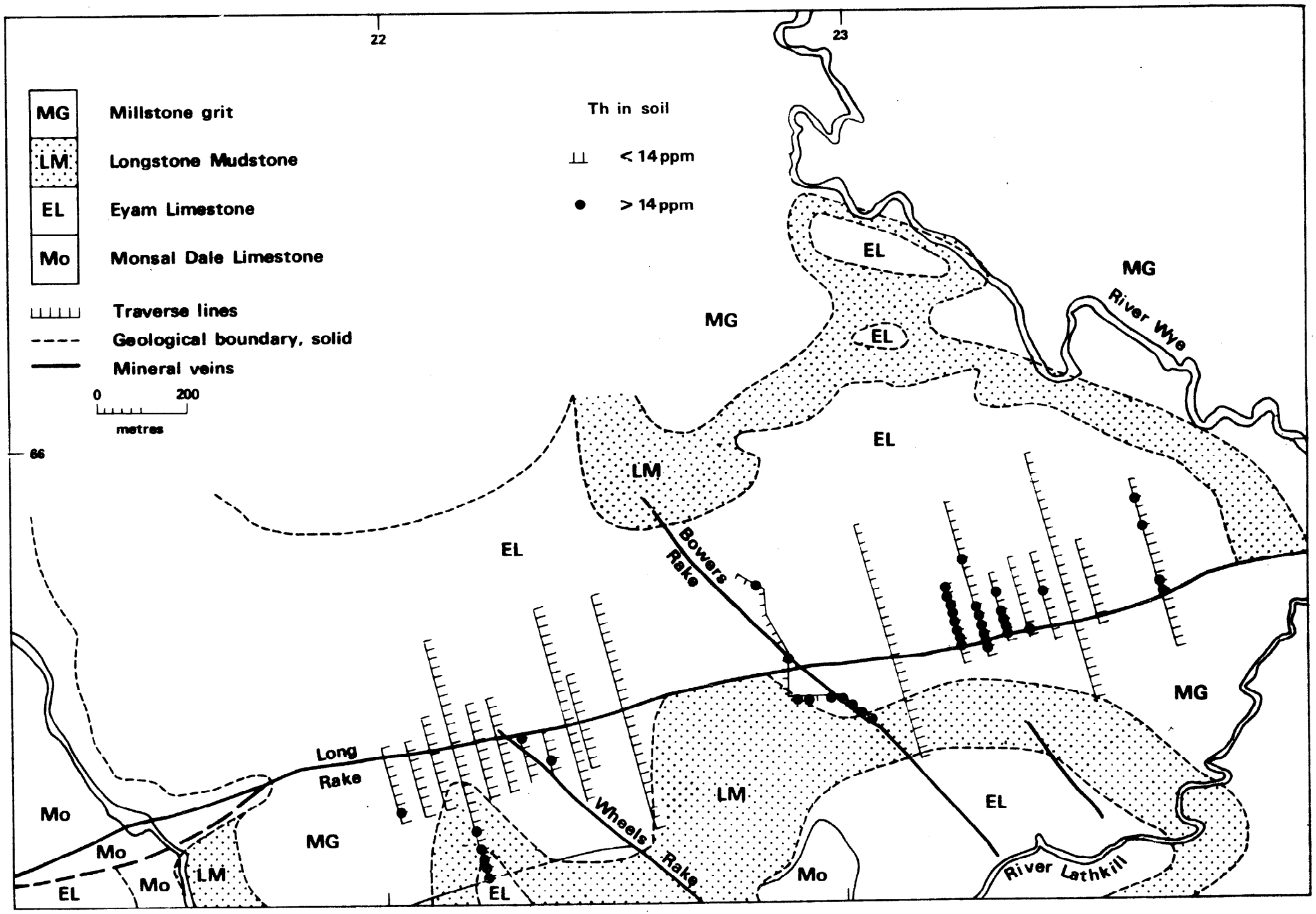
22
23
MG Millstone grit
LM Longstone Mudstone
EL Eyam Limestone
Mo Monsal Dale Limestone
Traverse lines
Geological boundary, solid
Mineral veins
0 200
metres
Th in soil
< 14 ppm
> 14 ppm
86
MG
EL
LM
Mo
River Wye
River Lathkill
Bowers Rake
Long Rake
Wheels Rake

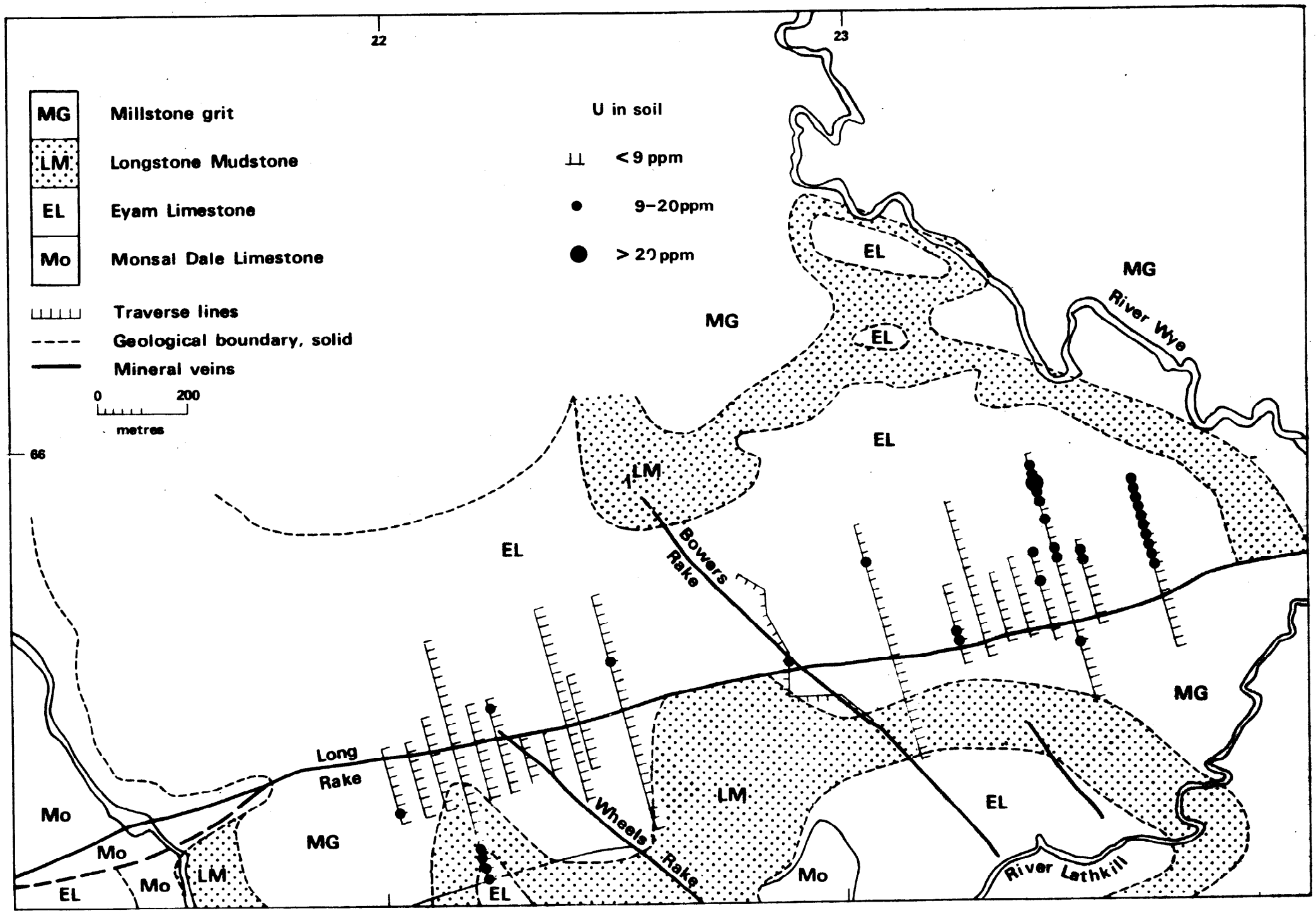
MG
Millstone grit
LM
Longstone Mudstone
EL
Eyam Limestone
Mo
Monsal Dale Limestone
Traverse lines
Geological boundary, solid
Mineral veins
0
200
metres
U in soil
< 9 ppm
9–20ppm
> 20 ppm
22
23
66
River Wye
Bowers Rake
Long Rake
Wheels Rake
River Lathkill

Appendix 3 Geological and gamma log for Borehole HF7

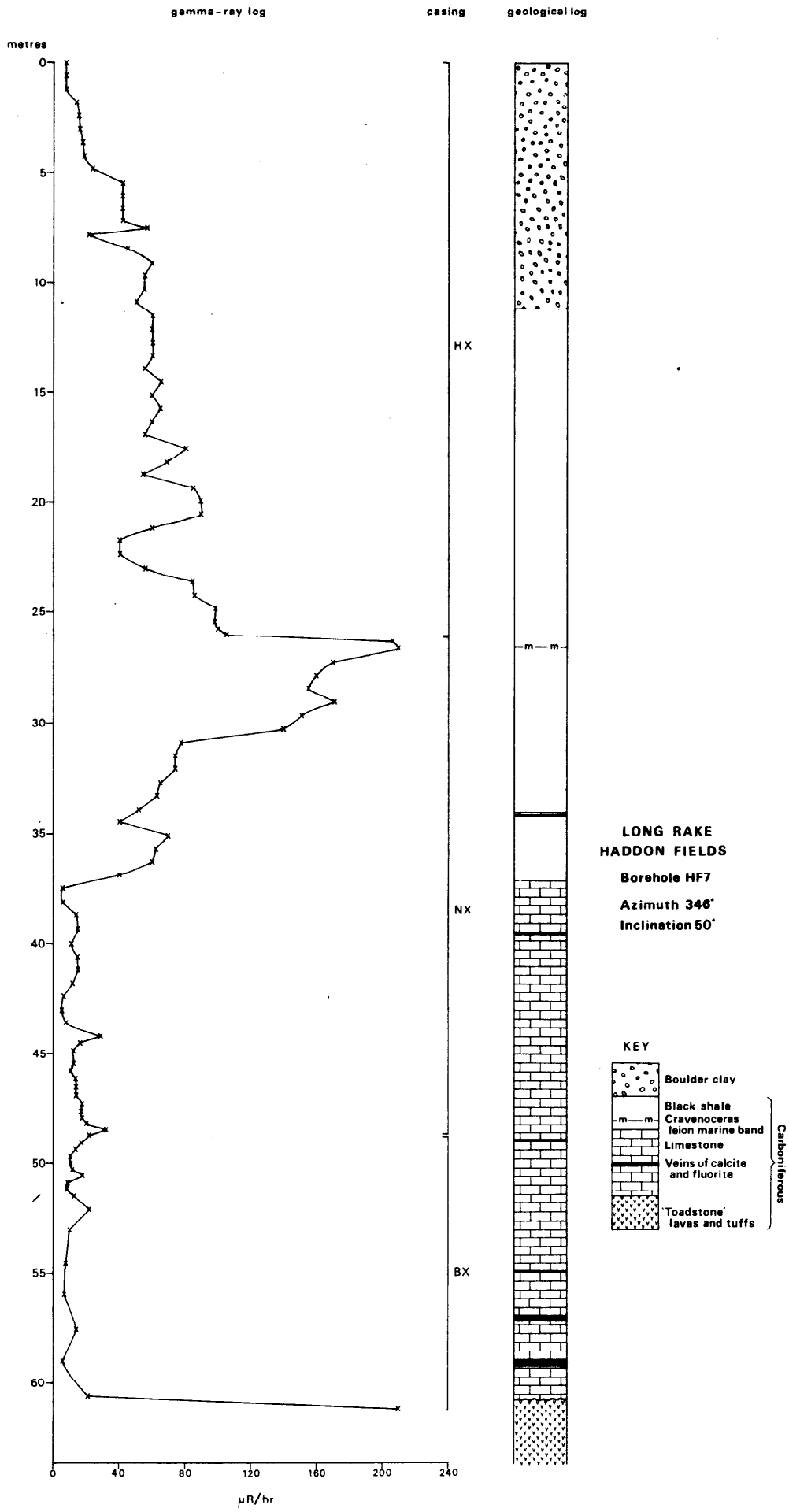

Appendix 4 Tabulated mineralogy of boreholes

No.	Depth m	Micritic	Fossiliferous	Stylolitic	Silicified	VEINS V_1 Carb.	VEINS V_2 Carb.	VEINS V_3 Fluorite	VEINS Barite	Sulphide	Hydrocarbon
Borehole HF4											
1	15.0		/								
2	16.0					/	/	/			
3	17.0										
4	18.0		/	/							
5	21.0		/	/		/					
6	24.0		/								
7	27.0		rare	/			/		/		
8	30.0	/	/	/			/			/	/
9	31.0	/	/	/			/	/			
10	32.0	/	/	/			/	/		/	/
11	33.0	/	/	/			/	/		/	
12	34.0	/					/	/			
13	35.0			/			/				
14	36.0			/		/					
15	37.0			/				/			
16	38.0			/			/				
17	39.0					/	/	/			
18	40.0										
19	41.0	/						/	/	/	
20	42.0		/				/	/	/	/	
21	43.0			/		/		/			
22	44.0			/		/		/			
23	45.0		/			/					
24	45.8			/			/	/			
25	46.0		/								
26	47.0	/	/	/	/		/	/			
27	48.0	/	/								
28	49.0							/			
29	50.0						/				
30	53.0	/	/	/			/	/	/	/	
31	56.0			/		/					
32	59.0						/				
33	62.0		/	/							
34	65.0	/		/			/			/	/
35	68.0		/	/		/					
37	74.0	/	/	/	/		/			/	/
38	77.0	/	/	/			/			/	/
Borehole HF5											
39	24.0		/					/			
40	30.0		/	/	/	/					//
41	31.0		/	/		/					
42	32.0		/	/			/	/			/
43	33.0		/	/		/					/
44	34.0		/	/		/					
45	34.4			/		/					
47	36.0		/		//	/					/
48	37.0	/	/	/	/	/	/			/	/
49	38.0			/		/					/
50	39.0			/		/	/				/
51	39.5						/	/		/PbS	
52	40.2	/		/		/	/	/			/
53	40.8			/		/	/	/		/PbS	/
54	41.9		/	/			/	/		/	/
55	42.0		/	/			/	/		/PbS	/
56	43.0	/	/	/	/	/				/	/
57	44.0	/	/	/		/	/	/			/
59	45.0		/			/	/	/			
60	46.0		/	/		/	/				
61	47.0	/	/				/	/		/	
62	48.0			/		/					/
63	49.0			/		/					/

No.	Depth m	Micritic	Fossiliferous	Stylolitic	Silicified	VEINS V_1 Carb.	VEINS V_2 Carb.	VEINS V_3 Fluorite	VEINS Barite	Sulphide	Hydrocarbon
64	50.0			/		/					/
65	54.0			/		/					/
66	**55.0**			/		/					/
67	56.0						/	/		/	
68	56.9						/	/			
69	57.0			/			/	/			/
70	58.0	/	/			/	/	/	/	/	/
71	59.0			/		/					/
72	60.0			/							/
73	61.0			/							/
Borehole HF1											
74	18.0					/					
75	21.0					/					
76	24.0		/								
77	25.0		/								
78	27.0		/	/							/
79	28.0					/					
80	29.0			/		/					/
81	30.0		/	/		/					/
82	31.0			/		/					
83	32.0			/		/					
84	33.0		/			/					
85	34.0			/		/	/				/
86	35.5					/					
87	37.0	/	/			/	/	/		/	/
88	38.0			/		/					
89	39.0							/	/	/	
90	40.0		/				/	/		/marcasite	/
91	41.0		/	/		/					
92	42.0						/	/			
93	43.0					/					
94	44.0	/	/								
95	45.0	/				/					
96	46.0		/	/		/					
97	47.0					/					
98	48.0			/		/					/
99	49.0					/					
100	52.0					/					
101	55.0					/					
102	58.0			/		/					
103	61.0	/	/	/		/				/	
104	64.0	/	/	/		/	/	/		/marcasite	